Fakultät für Medizin

Characterization of microRNA-365 and -29 and their effect on cardiac hypertrophy

Laurenz Noël Grüter

Vollständiger Abdruck der von der Fakultät für Medizin der Technischen Universität München zur Erlangung des akademischen Grades eines

Doktors der Medizin (Dr. med. sci.)

genehmigten Dissertation.

Vorsitzender: Priv.-Doz. Dr. Michael Joner

Prüfer der Dissertation:
1. Prof. Dr. Dr. Stefan Engelhardt
2. Assistant Prof. Dr. Alessandra Moretti

Die Dissertation wurde am 13.08.2018 bei der Technischen Universität München eingereicht und durch die Fakultät für Medizin am 20.02.2019 angenommen.

List of figures

Figure 1: “Conditions Leading to Remodeling of the Heart and Resulting in Atrophy or Hypertrophy.” (Hill and Olson 2008) 8
Figure 2: “The ‘linear’ canonical pathway of microRNA processing.” (Winter, Jung et al. 2009) 11
Figure 3: RNA-target recognition (Huntzinger and Izaurralde 2011) 13
Figure 4: human pre-miR-365a 15
Figure 5: miR-29 family gene clusters. 17
Figure 6: pENTR 1A-DF-Reporter. 26
Figure 7: Expression of miR-365 in NRCM and NRCF 38
Figure 8: miR-365 has a hypertrophic effect on NRCM. 39
Figure 9: miR-365 target screening. 40
Figure 10: binding sites for miR-365 in Cnot6l mRNA are highly conserved. 41
Figure 11: *Cnot6l* mRNA expression after transfection of miR-365 or antimiR-365. . 41
Figure 12: miR-365 directly regulates Cnot6l. 43
Figure 13: siRNA rescue hypertrophy assay. 45
Figure 14: miR-29 directly regulates *Ctnnbip1*. 47
Figure 15: miR-29 directly regulates *Glis2* 49
Figure 16: *Hbp1* is directly regulated by miR-29 50
Figure 17: The mammalian carbon catabolite repression 4 (CCR4) – negative on TATA-less (NOT) complex exerts deadenylase activities guided by RNA-binding proteins, miRISC and Tob (Shirai, Suzuki et al. 2014) ... 52
Figure 18: miR-365 CNOT6L negative feedback loop illustration 54
Figure 19: miR-29 directly regulates multiple members of the canonical Wnt-pathway in cardiac myocytes 57

Contents

List of figures 2

1 Introduction 6

1.1 Heart failure 6

1.1.1 Epidemiology 6

1.1.2 Clinical classification 6

1.1.3 Cardiac hypertrophy 7

1.2 MicroRNAs 9

1.2.1 Biogenesis 10

1.2.2 Mode of operation 11

1.3 MicroRNAs in the heart 13

1.4 miR-365 15

1.5 miR-29 17

1.6 Aim of the study 19

2 Materials and methods 20

2.1 Materials 20

2.1.1 Chemicals 20

2.1.2 Kits 20

2.1.3 Plasmids 20

2.1.4 Enzymes 21

2.1.5 Bacterial strains 21

2.1.6 Buffers and media 21

2.1.7 Oligonucleotide primers 22

2.1.8 microRNA precursors 23

2.1.9 antimiR molecules 24

2.1.10 Antibodies 24

2.2 Methods 25

2.2.1 In silico procedures 25

2.2.2 Generation of the double fluorescent reporter 25
2.2.3 RNA isolation 30
2.2.4 Reverse transcription of mRNA 30
2.2.5 Quantitative real time PCR of reversely transcribed mRNA 31
2.2.6 Reverse transcription of microRNA 32
2.2.7 Quantitative real time PCR of microRNA 33
2.2.8 Culture of HEK293 cells 33
2.2.9 Isolation of neonatal primary cells 33
2.2.10 NRCM hypertrophy assay 34
2.2.11 DF-reporter assay 36
2.2.12 Statistics 37
3 Results 38
3.1 miR-365 expression *in vitro* 38
3.2 microRNA-365 hypertrophic effect *in vitro* 38
3.3 miR-365 target evaluation 40
3.3.1 miR-365 *Cnot6l* regulation 41
3.3.2 miR-365 *Cnot6l* siRNA rescue 44
3.4 miR-29 target evaluation 45
3.4.1 miR-29 *Ctnnbip1* regulation 46
3.4.2 miR-29 *Glis2* regulation 47
3.4.3 miR-29 *Hbp1* regulation 49
4 Discussion 51
4.1 miR-365, Cnot6l and cardiac hypertrophy 51
4.1.1 miR-365 in cardiac hypertrophy 51
4.1.2 *Cnot6l*, the CCR4-NOT complex and cardiac hypertrophy 52
4.2 miR-29 and cardiac hypertrophy 54
4.2.1 Wnt signaling, *Ctnnbip1*, *Glis2* and *Hbp1* in the heart 54
4.2.2 miR-29 and Wnt signaling in the heart 56
4.2.3 miR-29 and cardiac hypertrophy and fibrosis 58
4.3 Conclusion 59
5 Summary 61

6 Zusammenfassung 62

7 Bibliography 63

8 Acknowledgments 77

1 Introduction

1.1 Heart failure

1.1.1 Epidemiology

For the past decade, cardiovascular diseases (CVDs) have been the main cause of death worldwide. They are responsible for 19% of global deaths under the age of 70 years (Organization 2014). In 2013, the first three top causes of death in Germany were associated with cardiovascular disease, i.e. chronic ischemic heart disease (8.2%), acute myocardial infarction (5.8%) and heart failure on position three (5.1%) followed by hypertensive heart disease on position seven (2.8%) and stroke on position eight (2.1%) (Bundesamt 2014). It is expected that CVD will remain the main cause of death worldwide by increasing from 16.7 million in 2002 to 23.3 million deaths in 2030 with ischemic heart disease as the main factor and hypertensive heart disease as an increasing reason for global mortality (Mathers and Loncar 2006).

1.1.2 Clinical classification

Chronic heart failure is the result of numerous pathologic mechanisms which cause a decreased pump function of the heart in the circulatory blood system. This leads to a lack of perfusion of downstream organs resulting subsequently in the decreased function or necrosis of the latter, commonly described as a forward failure (mainly symptomatic as a left ventricle failure). The New York Heart Association (NYHA) measures this effect as limited physical activity capacity to classify the heart failure (Little 1994). Moreover, the cardiac insufficiency as a backward failure, i.e., draining the venous system flowing into the ventricles, usually induces primarily symptoms, although those are less sensitive than diagnostic tools like echocardiography (Stevenson and Perloff 1989, Gopal and Karnath 2009).

In case of the left ventricle, these may be symptoms of the pulmonary system like dyspnea. Typically, these symptoms get aggravated by lying flat and improve while sitting up, called orthopnea. The symptoms induced by the forward failure of the left ventricle are for instance cool extremities, premature fatigue, dizziness, confusion, in advanced stages cyanosis and fading.

Symptoms of a backward failure of the right ventricle are peripheral edema, usually in the lower extremities, ascites and nocturia (Stevenson and Perloff 1989, Mueller, Frana et al. 2005, Gopal and Karnath 2009).
Beside the impaired pump function, heart failure changes the myocardial electrophysiological transmission, which may lead to arrhythmia (Hill and Olson 2008).

Risk factors respectively inducing stimuli for heart failure are age, male sex, hypertension, myocardial infarction (MI), coronary artery disease, valvular insufficiency and stenosis, congenital malformations, diabetes, obesity, smoking, chronic kidney disease and dyslipidemia (McKee, Castelli et al. 1971, Kannel and Belanger 1991, Bleumink, Knetsch et al. 2004, Kenchaiah, Narula et al. 2004, Schocken, Benjamin et al. 2008, Mahmood and Wang 2013, Yancy, Jessup et al. 2013, Bhatt, Foster et al. 2015).

1.1.3 Cardiac hypertrophy

The previously listed risk factors leading to heart failure emphasize the relevance of a chronic imbalance of supply and workload of the cardiac tissue (hypertension increases workload, ACS decreases the supply) which is usually evolving over time through the stages of cardiac hypertrophy.

To better understand pathologic cardiac hypertrophy, it is helpful to contrast it with physiologic hypertrophy which is usually induced by pregnancy and physical activity and can be restored entirely in absence of the inducing stimulus (Figure 1).

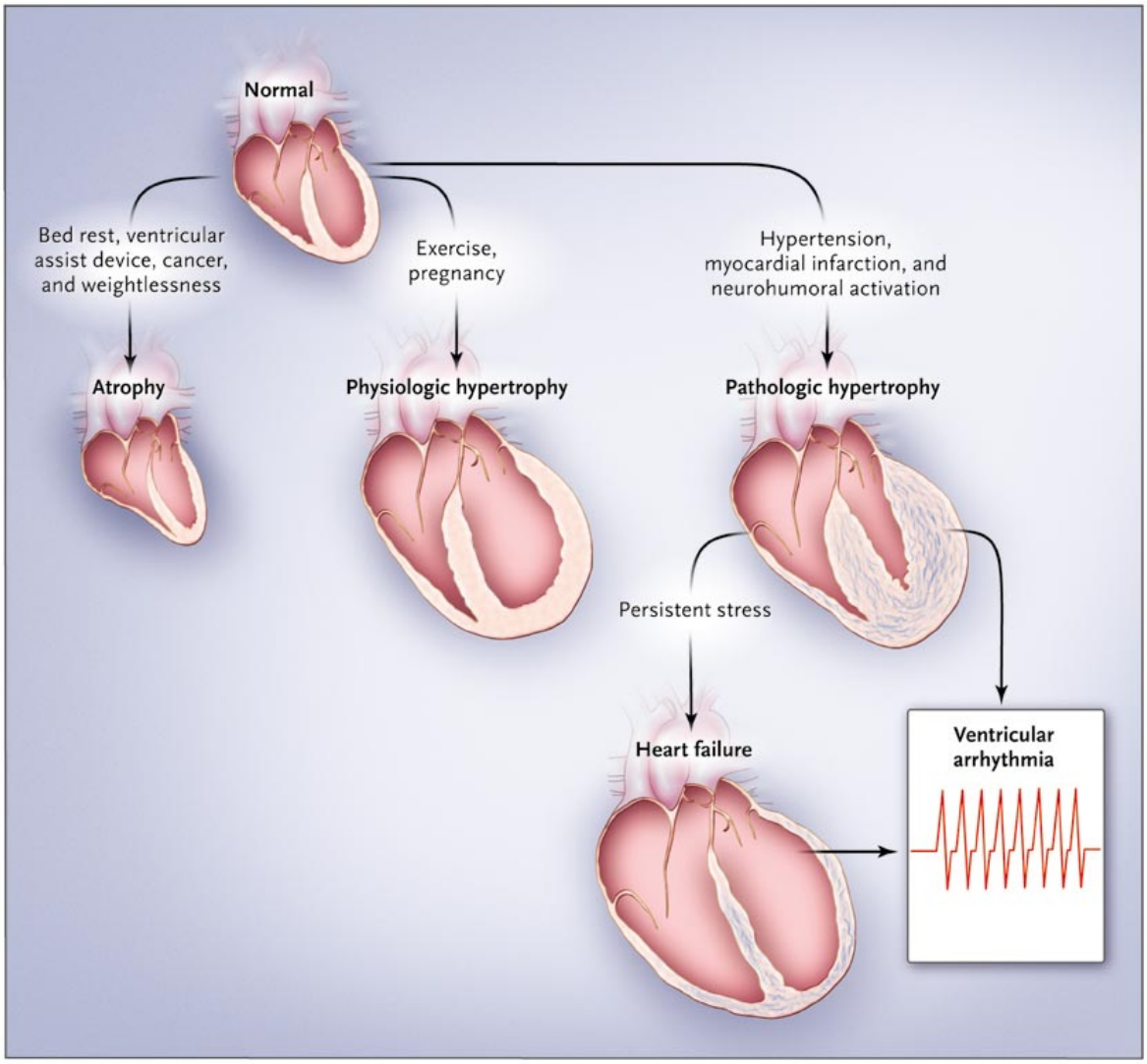

Figure 1: "Conditions Leading to Remodeling of the Heart and Resulting in Atrophy or Hypertrophy." (Hill and Olson 2008)

Microscopically, both forms of hypertrophy lead to an increased cardiomyocyte cell volume and production of new sarcomeres. However the pathologic hypertrophy can be identified by an unorganized sarcomere production, an additional cell necrosis and apoptosis with increased reactive intercellular fibrosis, summarized as cardiac remodeling (Grossman, Jones et al. 1975, Krayenbuehl, Hess et al. 1983, Weber, Clark et al. 1987, Pluim, Zwinderman et al. 2000, Brower, Gardner et al. 2006, McMullen and Jennings 2007).

Macroscopically, there are two forms of hypertrophy: concentric and eccentric hypertrophy. They are classified by the relation of the chamber volume to the wall

thickness. Both forms can describe pathologic and physiologic remodeling and should be understood as extreme examples with countless hybrid phenotypes in between. Pressure (over)load, induced by hypertension, aortic stenosis but also weight lifting can lead to concentric hypertrophy, characterized by a reduction of the ventricular volume-to-wall-thickness ratio.

Eccentric hypertrophy in contrast is typically caused by volume (over)load due to excessive endurance training or pregnancy as well as valvular insufficiency or cardiac shunts. It is marked by an increase of the ventricular volume-to-wall-thickness ratio and an absolute increase in ventricular mass.

If the wall thickness does not increase sufficiently according to the Laplace law, this leads to pathologic hypertrophy marked by cardiac dilation with increasing fibrosis, cell death and functional decompensation (Grossman, Jones et al. 1975, Krayenbuehl, Hess et al. 1983, Weber, Clark et al. 1987, Frohlich, Apstein et al. 1992, Hunter and Chien 1999, Pluim, Zwinderman et al. 2000, Brower, Gardner et al. 2006, McMullen and Jennings 2007, Hill and Olson 2008).

Functionally, pathologic hypertrophy leads to an impaired oxygen supply, contractility and diastolic and systolic function, whereas the physiological hypertrophy is associated with a preserved or increased pump function.

The pathological changes are mediated by intercellular communication and numerous neurohumoral factors. Furthermore, the tissue of a failing heart is marked by an altered genetic expression profile similar to the fetal heart. The exact regulation in the individual stages of cardiac hypertrophy and failure are yet to be understood more completely (Hunter and Chien 1999, Hill and Olson 2008, Dirkx, da Costa Martins et al. 2013).

1.2 MicroRNAs

MicroRNAs (in the following also referred to as miRs, miRNAs) are endogenous, genomically transcribed, short (20-23 nucleotides), non-coding, single-stranded RNA molecules which regulate gene expression in most animals post-transcriptionally (Bartel 2009). The crucial sequence for its functionality is found at the 5’ end from

nucleotide 2 to 7, called seed sequence, binding to the complementary sequence in the 3'UTR of its target mRNA (Brennecke, Stark et al. 2005, Bartel 2009, Pasquinelli 2012).

MiRBase (release 21, www.mirbase.org) has catalogued 2588 mature miRs in human (homo sapiens), 1915 in mouse (mus musculus), 765 in rat (rattus norvegicus) and 411 in pig (sus scrofa). There are microRNAs in plants, too, which presumably evolved independently from the animal's analogue, and are not to be discussed further in this study.

1.2.1 Biogenesis

Mammalian microRNA genes can be coded in several genomic contexts. In the following, the canonical pathway of microRNA biogenesis is described. Alongside this pathway, there are numerous variant mechanisms to be found, in their turn producing microRNAs (Yang and Lai 2011).

Most miRs are part of introns of a coding or noncoding transcript but can also be found in exons (Lagos-Quintana, Rauhut et al. 2001, Lau, Lim et al. 2001, Lee and Ambros 2001). Often their transcription is regulated together with the expression of their host genes, which can be related to their functional context. For instance, the myosin heavy chain gene Myh6 (α-MHC) cotranscribes miR-208a which controls the expression of other myosins (van Rooij, Quiat et al. 2009).

RNA Polymerase II or III transcribes them, producing primary microRNA transcripts of up to multiple kilobases length containing a typical stem-loop structure with the mature miR sequence, surrounded by single-stranded RNA segments on both 5' and 3' sides (pri-microRNAs) (Figure 2) (Lee, Kim et al. 2004, Borchert, Lanier et al. 2006). After transcription, the pri-miR gets cleaved by a nuclear RNase III (class 2) called Drosha – forming with its cofactor DGCR8 a complex named microprocessor – to release a hairpin structure of ~65 nucleotides (pre-miR) (Lee, Ahn et al. 2003, Gregory, Yan et al. 2004). The pre-miR then usually is translocated from the nucleus to the cytoplasm by exportin 5 with the cofactor Ran-GTP (Yi, Qin et al. 2003, Lund, Guttinger et al. 2004).

In the cytoplasm, the RNase III (class 3) called Dicer and optional cofactors cleave the pre-miR at the terminal loop to set free a short RNA duplex. In human, after cleavage

an Argonaute (AGO) protein binds the duplex forming the pre-RISC supported by the RISC loading complex (RLC) (Kawamata and Tomari 2010). Next, the duplex unwinds, supported by one of several helicases, into the guide and the passenger strand of the mature miR (also called miRNA and miRNA star (*)) (Meister, Landthaler et al. 2005, Robb and Rana 2007). The passenger strand is mostly discarded from the formed miRNA-induced silencing complex (miRISC) and degraded by nucleases. Therefore, in sequencing experiments, the guide strand accounts for 96-99% of both strands. Depending on whether it is the 5' or the 3' end of the precursor miR, the strand is called miR-…-5p or miR-…-3p (Lagos-Quintana, Rauhut et al. 2001, Lau, Lim et al. 2001, Okamura, Phillips et al. 2008).

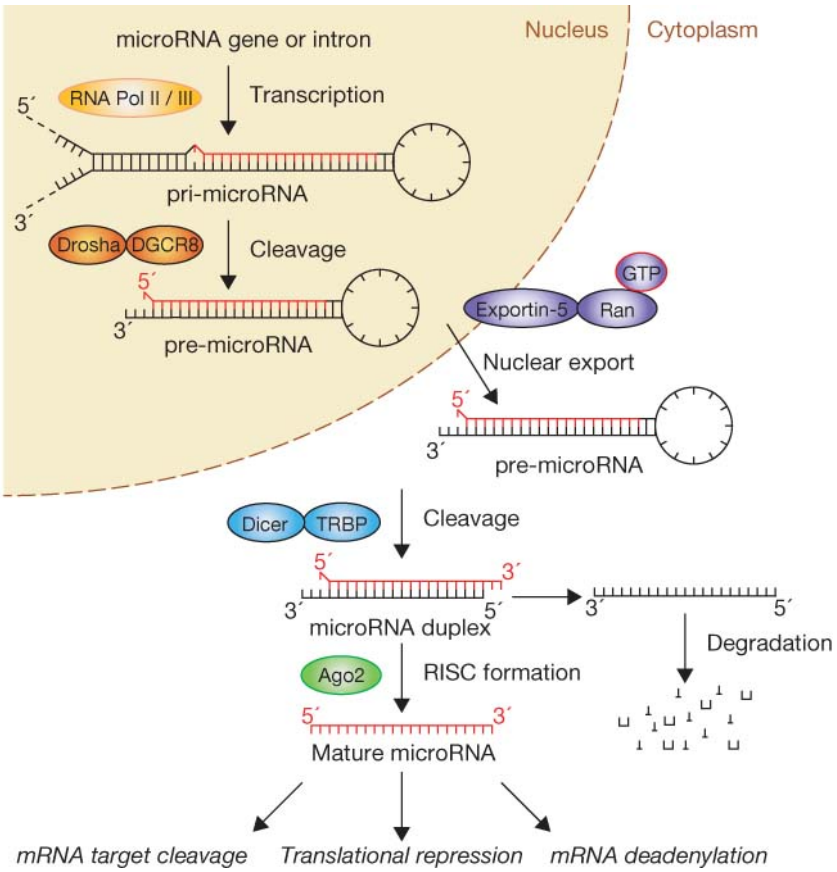

Figure 2: "The 'linear' canonical pathway of microRNA processing." (Winter, Jung et al. 2009)

1.2.2 Mode of operation

In cooperation with the miRISC, miRNAs can regulate target gene expression by cleavage, translational repression or mRNA deadenylation; which one of them occurs

depends on the AGO protein, which is part of the RISC, and on the level of fitting accuracy (Hutvagner and Zamore 2002, Yekta, Shih et al. 2004, Yu and Wang 2010). There are four different AGO proteins, AGO1 to 4. AGO2 is the only enzyme capable of cleaving RNA (Tolia and Joshua-Tor 2007). In addition to this regulation on the RNA level, there are reports that microRNAs can manipulate the DNA (Hwang, Wentzel et al. 2007, Benhamed, Herbig et al. 2012).

The classical understanding of the microRNA's mechanism of action considers the core seed region, i.e. nucleotide 2 to 7, as the complementary binding site for targets, leading to an inhibited target production by one of the three above mentioned mechanisms. In addition to the seed sequence, further complementarity of the microRNA seems to strengthen the binding effect to its target whereas perfect binding is not necessary for interaction between the mRNA and the microRNA, whether seed sequence or not. Such perfect or nearly perfect binding facilitates cleavage of the targeted mRNA. Translational repression, however, is achieved by less perfect target binding (Zeng and Cullen 2003).

Deadenylation is initiated in cooperation with GW182 proteins which recruit the PAN2-PAN3 and CCR4-CAF1-NOT deadenylase complexes (Braun, Huntzinger et al. 2011). The Cnot6l gene product Ccr4b is a subunit of the Ccr4-Not complex (Mittal, Aslam et al. 2011).

MicroRNA binding sites on mRNAs are typically found in the 3' untranslated region (UTR) (Lee, Feinbaum et al. 1993, Kuersten and Goodwin 2003).

Aside from its complementary binding efficacy, the abundance of a microRNA in a cell or cell compartment is crucial for the impact on its targets (Ameres and Zamore 2013).

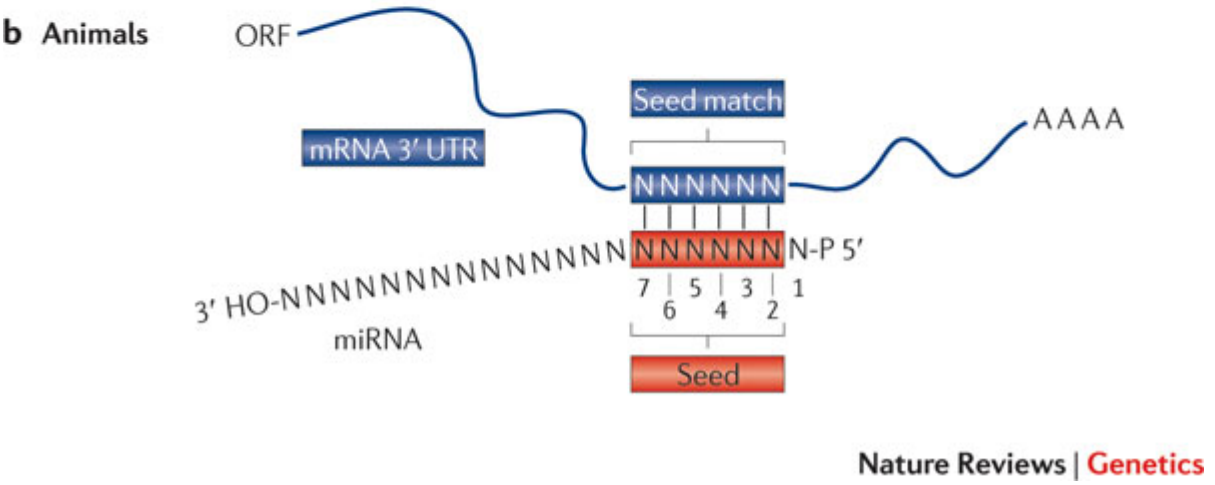

Figure 3: RNA-target recognition (Huntzinger and Izaurralde 2011)

1.3 MicroRNAs in the heart

As the first formed, most important supplying organ of the embryo that pumps oxygen- and nutrient-saturated blood originating from the placenta, the heart is essentially shaped under the influence of microRNAs (Olson 2006). This fact became obvious for the first time by means of cardiac-specific deletions of the RNase III Dicer, leading to dilated cardiomyopathy (DCM) and postnatal lethality, or outflow tract alignment and chamber septation disorders. It is assumed that 18 of the most abundant microRNAs in the heart account for over 90% of the cardiac microRNA pool (Chen, Murchison et al. 2008, Saxena and Tabin 2010).

After the embryologic development of the cardiovascular system, microRNAs play a vital role in the regulation to maintain the homeostasis in the cardiac tissue or to react on stimuli and change the genetic pattern, too. As noted above, miR-208a, cotranscribed with α-MHC, controls the expression of β-MHC, cotranscribing miR-208b, and Myh7b, cotranscribing miR-499. The balance of these myosins affects the contractility and pathological remodeling under stress conditions (van Rooij, Sutherland et al. 2007, van Rooij, Quiat et al. 2009). Hypertrophy can also be directly controlled by regulating signaling pathways in diverse cells of the cardiac tissue, like

the ERK-MAP kinase pathway in fibroblasts by miR-21 (Thum, Gross et al. 2008) or in cardiomyocytes by miR-378 (Ganesan, Ramanujam et al. 2013).

Recently there have been reports of microRNAs regulating cardiac rhythm on diverse levels (Kim 2013, Chiang, Zhang et al. 2015). MiR-1 has a proarrhythmogenic effect by targeting directly ion channel genes as KCNJ2 (a subunit the K^+ channel Kir2.1) and the connexin gene GJA1. MiR-1 is overexpressed in patients with coronary artery disease (Yang, Lin et al. 2007). SCN5A, a part of the Nav1.5 sodium channel, is directly and indirectly regulated by numerous microRNAs. miR-219, the only miR increasing SCN5A expression, abolished flecainide effects in mice (Daimi, Lozano-Velasco et al. 2015). The sodium-calcium exchanger 1 (NCX 1) is regulated by miR-135a, which is downregulated in mice with complete atrioventricular block (Duong, Xiao et al. 2017). MiR-106b and miR-93 (part of the miR-106b-25 Cluster) target the ryanodine receptor type II (a sarcoplasmic reticulum Ca^{2+} channel). Loss of this cluster and overexpression of this channel contribute to atrial fibrillation (Chiang, Kongchan et al. 2014). Another gap junction protein, connexin 43, is directly regulated by miR-130a. Loss of this transmembrane protein leads to diverse atrial and ventricular arrhythmias (Osbourne, Calway et al. 2014).

Several microRNAs have been shown to regulate the different stages of reaction on acute myocardial infarction (Boon and Dimmeler 2015). For example inhibition of miR-34a reduces cell death, fibrosis and improves myocardial contractility after infarction (Boon, Iekushi et al. 2013). Furthermore, it has been shown that numerous microRNAs regulate angiogenesis following myocardial infarction (Bonauer, Carmona et al. 2009, Hullinger, Montgomery et al. 2012, Iaconetti, Polimeni et al. 2012).

More recent findings indicate that microRNAs also contribute to paracrine communications in the heart as regulators of secreted factors and as secreted “mircrines” themselves. Moreover, there are microRNAs circulating in the blood with a diagnostic and prognostic relevance for heart diseases like the acute coronary syndrome (ACS) (Widera, Gupta et al. 2011, Hergenreider, Heydt et al. 2012, Viereck, Bang et al. 2014).

1.4 miR-365

The miR-365 family is conserved in several species. For instance, miR-365 has two genomic transcripts in human and mouse, and one transcript in rat. One of the transcripts, called miR-365a in human and miR-365-1 in mouse, is encoded on chromosome 16 in an intergenic context clustered with miR-193b (separated by 5236 bp (base pairs) in human). The other transcript is called miR-365b in human or miR-365-2 in mouse respectively and is encoded on chromosome 17 for human and chromosome 11 for mouse in an intergenic context. In human, it is transcribed in a cluster with miR-4725 separated by 53 bp. In the rat genome, miR-365 is encoded on chromosome 10. In all three species, the 5p strand is described as the star strand, so the 3p strand, which is included in the RISC, is considered as the strand of interest in this study (Figure 4). These strands all share the same sequence. In the heart, hsa-miR-365a was ranked by abundance in a RNA sequencing study at position 133 of 815 (b on position 160), mmu-miR-365-1 was at position 239 of 583 (2 on position 260) (Meunier, Lemoine et al. 2013).

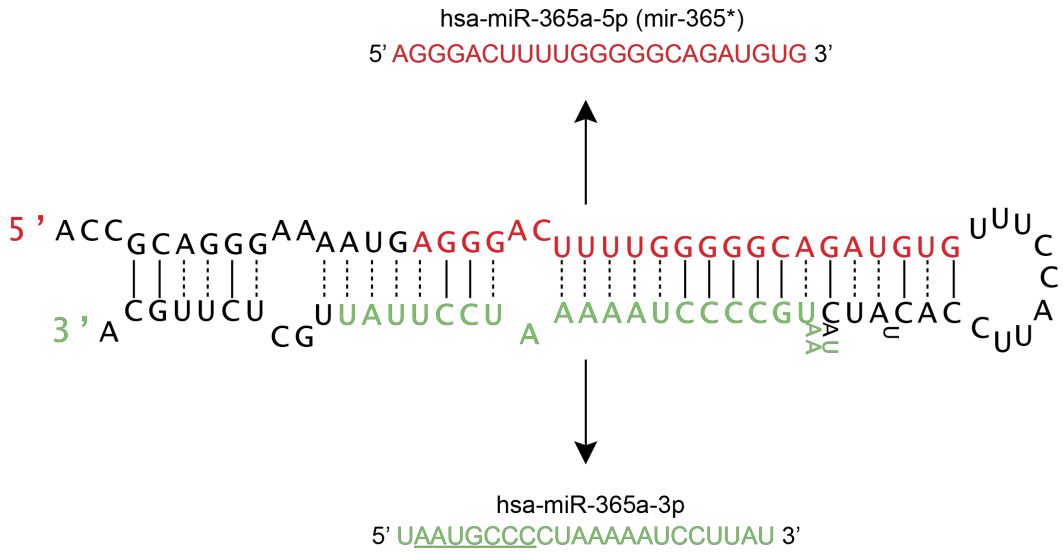

Figure 4: human pre-miR-365a. cleaved into its products, the guide strand (3p) and the passenger strand (5p/*); The underlined region of the 3p strand displays the seed region.

Little is known about the effects of miR-365 in a healthy heart and in a heart under pathologic conditions. MiR-365 has been found to have a strong hypertrophic effect in

neonatal rat cardiac myocytes in a phenotype screening study (Jentzsch, Leierseder et al. 2012). Also, its expression seems to be strongly upregulated in the remote myocardium of a murine myocardial infarction (MI) model and human heart failure (Small, Frost et al. 2010). Recently it has been suggested that miR-365 regulates cardiac hypertrophy by inhibiting Skp2 expression, which promotes autophagy. The same study observed an upregulation of miR-365 in cardiac hypertrophy (Wu, Wang et al. 2017). Another study found miR-365 to be downregulated in patients with coronary atherosclerosis (Lin, Feng et al. 2016).

Until lately, MiR-365 has been investigated mostly in context of carcinogenesis as a tumor suppressor. It targets cyclin D1 and cdc25A in gastric cancer (Guo, Ye et al. 2013), cyclin D1 and Bcl-2 in colon cancer (Nie, Liu et al. 2012), thyroid transcription factor 1 (TTF-1, also called NKX2-1) in lung cancer (Qi, Rice et al. 2012, Kang, Lee et al. 2013), the small GTPase Rasd1 in murine embryonic fibroblasts (Xiong, Jung et al. 2015), interleukin 6 (IL-6) in breast cancer metastasis (Xu, Xiao et al. 2011, Hong, Li et al. 2015) and restored the p27/Myc/phosphor-Rb signature back to normal levels in breast and ovarian cancer cells (Seviour, Sehgal et al. 2015).
Without any assumed or proven target gene, it has also been found that miR-365 blocks cancer cell proliferation and migration in hepatocellular carcinoma (HCC) (Chen, Huang et al. 2015). MiR-365 promotes chondrocyte differentiation by targeting histone deacetylase 4 (HDAC4) (Guan, Yang et al. 2011).

In opposition to these studies describing miR-365 as a tumor suppressing miRNA, there are studies which show a tumor promoting effect.
MiR-365 inhibits NFIB in cutaneous squamous cell carcinoma (Zhou, Liu et al. 2013, Zhou, Zhou et al. 2014) and the pro apoptotic protein BAX and the adaptor protein SHC1 in pancreatic cancer cells (Hamada, Masamune et al. 2014).

Another field of investigation is the effect of miR-365 in cell differentiation to brown adipose tissue. It has been shown that miR-365 can indeed promote this process in cooperation with other miRNAs, albeit not being vital to it (Feuermann, Kang et al. 2013, Mori, Thomou et al. 2014).

1.5 miR-29

The miR-29 family consists of four members organized in two bicistronic clusters in human. One cluster on chromosome 7 in human and mouse respectively chromosome 4 in rat encodes miR-29a and miR-29b-1. The other cluster on chromosome 1 in human, mouse and rat encodes miR-29c (in rat called miR-29c-1) and miR-29b-2.
In all species for all family members, the 3p-strand is considered as the guide strand. They all share the same seed sequence (Figure 5). In the heart, the miR-29 family is highly expressed. Hsa-miR-29c was ranked by abundance in a RNA sequencing study at position 30 of 815 (a on position 73), mmu-miR-29a was at position 19 of 583 (c on position 21) (Meunier, Lemoine et al. 2013).

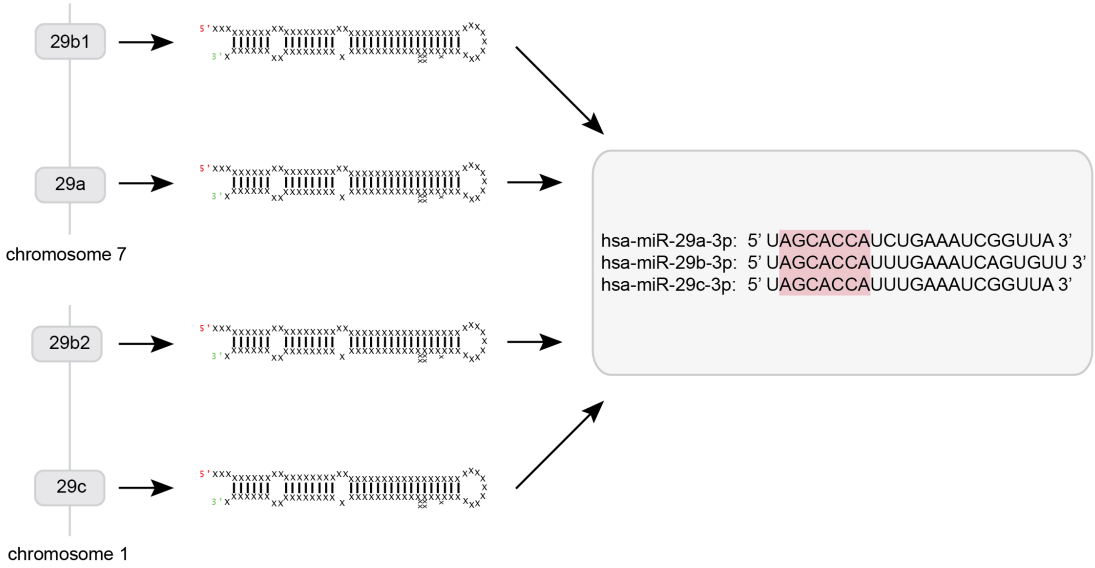

Figure 5: miR-29 family gene clusters. pre-miRs in hairpin structure; mature microRNAs; All family members share the same seed sequence (highlighted in red).

In scientific literature, the miR-29 family is majorly associated with inhibition of fibrosis in diverse organs (Ramdas, McBride et al. 2013, Cushing, Kuang et al. 2014, Montgomery, Yu et al. 2014, Meng, Tang et al. 2015, Zanotti, Gibertini et al. 2015). This effect is thus concordantly described in the heart as well. Van Rooij found miR-29 to be downregulated in the border zone of the infarcted area and the remote myocardium three days and 14 days after MI. Furthermore, the miR-29 family expression in cardiac myocytes is dependent on phenylephrine (PE). In cardiac

fibroblasts, it seemed to be 5- to 12-fold more expressed. It was shown that several extracellular matrix proteins, e.g. COL1A1, COL1A2, COL3A1 and fibrillin, are targets of miR-29 and accordingly more expressed in fibrotic remodeling. While a knockdown of miR-29b via an antagomiR increased collagen mRNA *in vivo*, an overexpression with a miR-29b mimic in fibroblast culture led to reduced collagen mRNA expression (van Rooij, Sutherland et al. 2008, Abonnenc, Nabeebaccus et al. 2013).
Transforming growth factor β (TGFβ) repressed miR-29 via Smad3. MiR-29 reduced downstream Wnt pathway members and collagen expression in orbital fibroblasts (Tan, Tong et al. 2014). The assumed protective effect of miR-29b on fibrotic remodeling of the heart could recently be shown in a murine Angiotensin II induced hypertension model (Zhang, Huang et al. 2014). Another study showed an upregulation of miR-29c after triiodothyronine injection in an ischemia/reperfusion model leading to reduced remodeling (Nicolini, Forini et al. 2015). Interestingly, overexpression of the miR-29 family led to loss of myofibril bundles in diabetic rats through its target Mcl-1 (see below), showing a suppression mechanism by insulin (Arnold, Koppula et al. 2014). Consistent with following paragraph about neoplastic processes, miR-29a inhibits H9c2 (rat cardiac myoblasts) cell proliferation by targeting cyclin D2. Conversely, miR-29a inhibition leads to increased proliferation (Cao, Wang et al. 2013). However, a phenotypic screening of our research group showed the miR-29 family as hypertrophic microRNAs in neonatal rat cardiac myocytes (Jentzsch, Leierseder et al. 2012).

Another field of study is the role of miR-29 in carcinogenesis. MiR-29 seems to possess to a large extent a tumor suppressing effect and is accordingly downregulated in neoplastic tissue. This effect is achieved by targeting DNA methyltransferases which secondarily inhibit tumor suppressors (Fabbri, Garzon et al. 2007). Moreover, miR-29 has a pro-apoptotic effect by targeting Mcl-1, secondarily controlling Bcl-2, p85a and CDC42, which regulate p53 (Mott, Kobayashi et al. 2007, Park, Lee et al. 2009). It can lead to cell cycle arrest by targeting cyclin E (beside the mentioned cyclin D2 regulation) (Ding, Chen et al. 2011).
In terms of cell migration, there are reports which show an inhibiting or a reinforcing effect by miR-29 by regulating matrix metalloproteinases or inter alia collagens (Rothschild, Tschan et al. 2012, Wang, Gao et al. 2012). A migration and metastasis

promoting role of miR-29 is supported by the observation that miR-29 mediates epithelial-mesenchymal-transition (Gebeshuber, Zatloukal et al. 2009).

1.6 Aim of the study

Cardiovascular diseases are the main cause of death worldwide. In Germany, heart failure is the third most frequent cause of death following chronic ischemic heart disease and MI. In the past two decades, it has been become progressively evident that posttranscriptional gene regulation by microRNAs has a great impact on biological processes and diseases. Yet, understanding the pathologic mechanisms of heart failure requires more information on microRNAs orchestrating structural, hormonal and functional modifications to this disease.

The miR-29 family has been shown to have several effects on diverse tissues and organs by targeting and regulating numerous genes and pathways. Some studies suggested an antifibrotic and an antiproliferative effect of miR-29 in the heart by targeting multiple collagens and cell cycle pathways. However, our group has previously identified miR-29 and miR-365 as one of the most potent hypertrophic microRNAs in isolated cardiac myocytes (Jentzsch, Leierseder et al. 2012). Subsequently, this study aimed to investigate the function and mechanism of action of both microRNAs in cardiac tissue.

2 Materials and methods

2.1 Materials

2.1.1 Chemicals

Chemical	Manufacturer
5-bromodeoxyuridine (BrdU)	Sigma-Aldrich (Deisenhofen)
Agarose	Peqlab (Erlangen)
Chloroform	Roth (Karlsruhe)
Deoxynucleotide triphosphate (dNTP)	Life Technologies (Carlsbad, USA)
DNase/RNase free water	Gibco (Karlsruhe)
Dulbecco's modified eagle medium (DMEM)	Gibco (Karlsruhe)
Dulbecco's phosphate buffered saline (DPBS)	Gibco (Karlsruhe)
Ethanol	J.T. Baker (Phillipsburg, USA)
Ethidium bromide	Sigma-Aldrich (Deisenhofen)
Fetal bovine serum (FBS) = fetal calf serum (FCS)	PAN (Aidenbach)/ Gibco (Karlsruhe)
Glycerol	Merck (Darmstadt)
HEPES	Applichem (Darmstadt)
Isopropanol	Merck (Darmstadt)
L-glutamine	Life Technologies (Carlsbad, USA)
Lipofectamine™ 2000	Life Technologies (Carlsbad, USA)
Paraformaldehyde (PFA)	Sigma-Aldrich (Deisenhofen)
Penicillin/Streptomycin	Gibco (Karlsruhe)
PeqGOLD Trifast™	Peqlab (Erlangen)
Phenol/chloroform	Roth (Karlsruhe)
Phenylephrine (PE)	Sigma-Aldrich (Deisenhofen)
S.O.C. medium	Life Technologies (Carlsbad, USA)
Triton™ X-100	Sigma-Aldrich (Deisenhofen)

2.1.2 Kits

Kit	Manufacturer
EndoFree Plasmid Maxi Kit	Qiagen (Hilden)
FastStart Universal SYBR Green Master (Rox)	Roche (Basel)
miRCURY LNA™ Universal RT microRNA PCR kit	Exiqon, now Qiagen (Hilden)
QIAquick Gel Extraction kit	Qiagen (Hilden)

2.1.3 Plasmids

Plasmid	Reference
pENTR-1A-DF-reporter	Stanislas Werfel (IPT, TUM, Munich)

2.1.4 Enzymes

Enzyme	Manufacturer
Accuprime Pfx DNA Polymerase + 10X Accuprime Pfx Buffer	Life Technologies (Carlsbad, USA)
Benzonase	Sigma-Aldrich (Deisenhofen)
Collagenase II	Worthington (Lakewood, USA)
Proteinase K	Fermentas (St. Leon-Rot)
Restriction endonucleases + corresponding buffers	New England Biolabs (Frankfurt am Main)
SuperScript™ II RT + corresponding buffer	Life Technologies (Carlsbad, USA)
T4 DNA Ligase + 10x Ligase Buffer	New England Biolabs (Frankfurt am Main)
Taq DNA polymerase + corresponding buffer	Fermentas (St. Leon-Rot)

2.1.5 Bacterial strains

bacterium	Manufacturer
E. coli DH10B (electrocompetent)	Life Technologies (Carlsbad, USA)

2.1.6 Buffers and media

Buffer/medium	Ingredients	Amount
BrdU stock	BrdU ddH_2O	230 mg 74.8 ml
Buffer P1	Tris EDTA Rnase I	50 nM 10 nM 100 mg pH adjusted to 8.0
Buffer P2	NaOH SDS	200 mM 1%
Buffer P3	Potassium acetate	3 M pH adjusted to 5.5
Buffer TAE (50x)	Tris Acetic acid EDTA disodium salt ddH_2O	242 g 57.1 ml 37.2 g to 1 l
DNA lysis buffer	Tris EDTA NaCl	2.1 g 1.87 g 11.7 g

	SDS ddH_2O	0.2 g to 1 l
LB agar	Peptone Yeast extract NaCl Agar NaOH (1 M) ddH_2O	10 g 5 g 5 g 15 g 1 ml to 1 l
LB medium	Peptone Yeast extract NaCl NaOH (1 M) ddH2O	10 g 5 g 5 g 1 ml to 1 l
NRCM incomplete medium	MEM $NaHCO_3$ vitamin B12 ddH_2O	10.7 g 0.35 g 1 ml to 1 l pH adjusted to 7.3 and sterile filtered
PBS (10x)	NaCl KCl $Na_2HPO_4.7H_2O$ KH_2PO_4 ddH_2O	80 g 2 g 11.5 g 2 g to 1 l
Primary cell media	FBS Penicillin/Streptomycin BrdU stock NRCM incomplete medium	ml ≙ % 1 ml (if not noted otherwise) 1 ml (for CM culture) to 100 ml

2.1.7 Oligonucleotide primers

a) Cloning primers

All primers were manufactured by Sigma-Aldrich (Deisenhofen) in HPSF-purified lyophilized powder. The oligonucleotides were dissolved with double-distilled autoclaved water to a 1 mM concentration by keeping it for 10 min at 55°C and 700 rpm. For the experiments 20 µM working solutions were used.

Gene	Sequence (5'-3')
Cnot6l 3'UTR	AAAAAAACCGGTGGCACTCTGTTGCAAGAAGG (forward) AAAAAACAATTGCCCAACACACCTCAGCTTCT (reverse)
Glis2 3'UTR	AAAAAAACCGGTCCCGACGAACAGAAACTC (forward) AAAAAACAATTGACTCTAAGGCCAGCAGTC (reverse)
Hbp1 3'UTR	AAAAAAACCGGTGGTGAGGATTGCTTTCTCCA (forward) AAAAAAGAATTCACATGAGGGTATGTGGCTGAGG (reverse)
Ctnnbip1 3'UTR	AAAAAAACCGGTGGTAGCAAACCACCGTCTTC (forward) AAAAAAGAATTCCCAAACCCTGTTTTCTGCTT (reverse)

b) qPCR mRNA primers

Gene	Sequence (5'-3')
Cnot6l rno	CGGGTGTTGCCTTATGAACT (forward) GGAAGCTGCTCTGGATGAAC (reverse)
Glis2 rno	CTATCAGGCTTGGGAAGCAG (forward) TGCTCCATGTCTAGGCCTCT (reverse)
Hbp1 rno	AAGGCTTTGGCTGAAGAACA (forward) AGCTTTTCCGTCCAGAGTCA (reverse)
Ctnnbip1rno	TCCGAGCTCTGGTGCTTTAT (forward) CCAAACCCTGTTTTCTGCAT (reverse)
Gapdh rno	ACAACTTTGGCATCGTGG (forward) AGTGGATGCAGGGATGATGT (reverse)

c) qPCR microRNA primers

All microRNA qPCR primers were manufactured by Exiqon as a miRCURY LNA™ Universal RT microRNA PCR LNA™ PCR primers set. All primers are compatible to homo sapiens, mus musculus and rattus norvegicus species.

microRNA	Sequence (5'-3')
hsa-miR-365-3p	UAAUGCCCCUAAAAAUCCUUAU
Control = U6	Product No.: 339306; Cat. No.: YP00203907

2.1.8 microRNA precursors

MicroRNA precursor molecules were manufactured by Ambion® Life Technologies. All precursors are applicable for use in homo sapiens, mus musculus and rattus norvegicus species.

microRNA	Sequence (5'-3')
hsa-miR-365-3p	AGAGUGUUCAAGGACAGCAA GAAAAAUGAGGGACUUUCAG GGGCAGCUGUGUUUUCUGAC UCAGUCAUAAUGCCCUAAA AAUCCUUAUUGUUCUUGCAG UGUGCAUCGGG (stem loop)
hsa-miR-29a-3p	AUGACUGAUUUCUUUUGGUG UUCAGAGUCAAUAUAAUUUU CUAGCACCAUCUGAAAUCGG UUAU (stem loop)
hsa-miR-29b-3p	CUUCUGGAAGCUGGUUUCAC AUGGUGGCUUAGAUUUUUCC AUCUUUGUAUCUAGCACCAU UUGAAAUCAGUGUUUUAGGA G (stem loop)
hsa-miR-29c-3p	AUCUCUUACACAGGCUGACC GAUUUCUCCUGGUGUUCAGA GUCUGUUUUUGUCUAGCACC AUUUGAAAUCGGUUAUGAUG UAGGGGGA (stem loop)
Control	(Pre-miR™ miRNA Precursor Negative Control #1 AM17110 (Thermo Fisher Scientific))

2.1.9 antimiR molecules

All antimiR molecules were manufactured by Exiqon as miRCURY LNA™ microRNA inhibitors.

microRNA	Sequence (5'-3')
mmu-miR-365-3p (18mer, *in vitro*)	TTACGGGGATTTTTAGGA
mmu-miR-29-3p	GATTTCAAATGGTGCT
Negative control	TCAGTATTAGCAGCT

2.1.10 Antibodies

Antibody	Manufacturer
4′,6-Diamidine-2′-phenylindole dihydrochloride (DAPI)	Sigma-Aldrich (Deisenhofen, Germany)
Alexa488 goat anti-mouse IgG	Life Technologies (Carlsbad, USA)
Monoclonal mouse α-actinin	Sigma-Aldrich (Deisenhofen, Germany)

2.2 Methods

2.2.1 In silico procedures

The cloning process was planned with the software MacVector 12.0.6 (Cambridge, UK). All primers were designed with primer3plus (http://www.bioinformatics.nl/cgi-bin/primer3plus/primer3plus.cgi) and the alignment was checked with BLAST (https://blast.ncbi.nlm.nih.gov/Blast.cgi). MicroRNA targets were searched via targetscan (Release 7.1, http://www.targetscan.org/). Sequences and templates were gathered from MiRBase (Release 21, http://www.mirbase.org/), ensemble (http://www.ensembl.org/index.html) and NCBI (https://www.ncbi.nlm.nih.gov/).

2.2.2 Generation of the double fluorescent reporter

The double fluorescent reporter plasmid pENTR-1A-DF-Reporter scaffold was designed and provided by Stanislas Werfel (IPT, TUM, Munich; Figure 6). The 6229bp long plasmid contains two antidromically arranged CMV promoters. Behind each, there is either the sequence of EGFP or tdTomato. Downstream of EGFP, there are the restriction sites of AgeI, EcoRI and MfeI which were used for inserting the 3'UTR of interest. There is a Kanamycin resistance gene present, too, which is needed for positive selection (of bacterial clones which possess and transcribe this plasmid).

Briefly explained, two products of this plasmid are transcribed: the tdTomato, a red fluorescent protein, and the EGFP, a green fluorescent protein. Attached to the end of the open reading frame of the EGFP, there is the 3'UTR which needs to be investigated. If the applied (and investigated) microRNA binds to this 3'UTR, this leads to a decreased translation of the EGFP mRNA, resulting in a reduced ratio of GFP to RFP. This effect is measurable via microscopy for each cell individually.

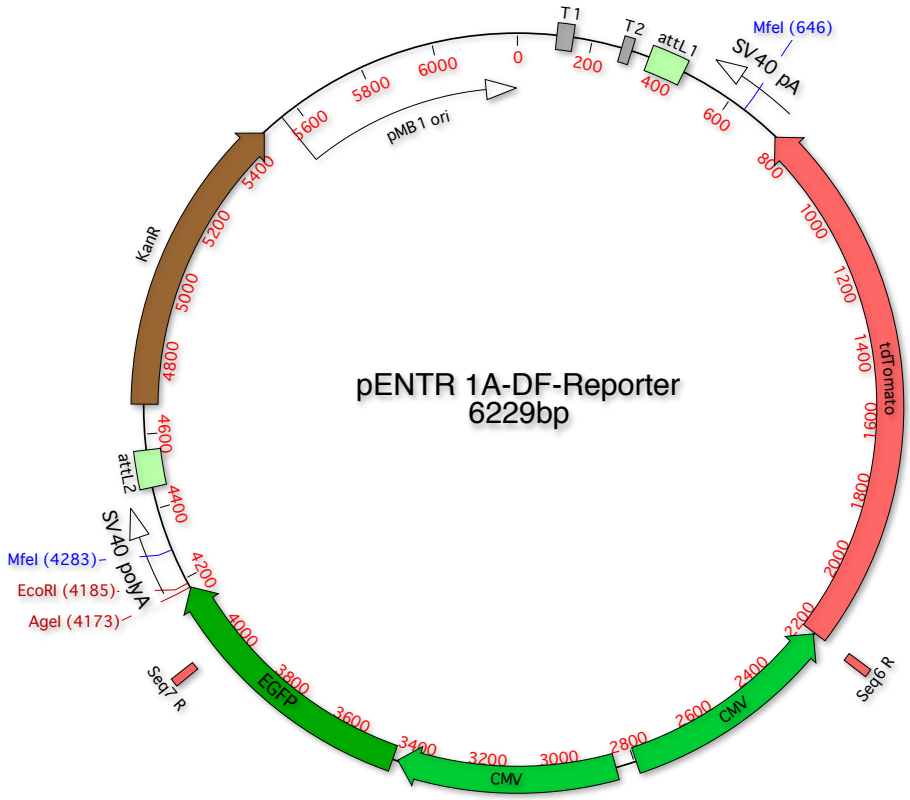

Figure 6: pENTR 1A-DF-Reporter. the 6229bp long plasmid contains two antidromically arranged CMV promoters. Behind each, there is either the transcription of EGFP or tdTomato. Downstream of EGFP, there are the restriction sites of AgeI and EcoRI (picture created using MacVector).

a) 3'UTR insert amplification via PCR

To create the 3'UTR insert for the reporter scaffold, primers were designed to duplicate a region containing all potential binding sites of the investigated microRNA plus a minimum border zone of 200bp length. The primers contained either AgeI for the forward primers and EcoRI or MfeI restriction sites for the reverse primers. To ensure an efficient digestion, 4-8bp were added in front of the restriction sites at the 5' end. As a template for the inserts served the genomic DNA of tail ends of male C57BL/6N mice (Charles River Laboratories).

The following reagents were used for amplification via PCR:

Reagent	Amount
10X Accuprime Pfx Buffer	5 µl
Forward primer	20 pmol
Reverse primer	20 pmol
Template DNA	100 - 200 ng
Accuprime Pfx DNA Polymerase	2.5 units
DNase/RNase free water	to 50 µl

The thermal cycling program below was used:

Stage	Step	Duration	Temperature	Cycles
1	Polymerase Activation	2 min	95° C	1
2	Denaturation	15 s	95° C	35
	Annealing/Extension	30 s	55-65° C	
	Extension	1 min per kb	68° C	
3	Final extension	5 min	68° C	1

b) Gel electrophoresis

The PCR products were afterwards assorted by electrophoresis in 1% agarose gel and visualized with ethidium bromide under ultraviolet light to excise the gel region containing the correct PCR product. Ethidium bromide intercalates into DNA. As a fluorescent molecule, it helps visualizing these molecules under UV light with a wavelength of 312 nm.

The first step was to prepare the gel with 1g of agarose in 100 ml of 1X TAE buffer. Afterwards, the mixture was heated in a microwave oven for 2 minutes. Then, after cooling the mix to 50°C, 10 ml ethidium bromide were added to 100 ml of the solution (0.1 µg/µl). The fluid was thus poured into the gel tray with the fitting comb (Peqlab). 5x DNA loading buffer was added to the PCR products in the correct amount and injected the mix into the wells. 100 bp and 1 kb DNA ladders (New England Biolabs (Frankfurt am Main)) were applied as a reference. The gel trays were placed into the chambers filled with 1x TAE buffer and a voltage of 70 – 140 V was applied for 20-40 min. Lastly, the gel was placed under UV light (DeVision, Decon Science Tec DBOX, Hohengandern) to visualize the band structures and the gel region of interest was excised.

c) Gel extraction of the DNA

The procedure was to use a QIAquick Gel Extraction Kit (Qiagen, Hilden) to extract the DNA from the gel. First, three volumes of Buffer QG was added to one volume of gel and incubated the tube containing both at 50° C for 10 minutes to dissolve the gel. Second, one gel volume of isopropanol was added to the sample and mixed. The mix was then transferred to a QIAquick spin column and centrifuged for 1 minute at 13.000 rpm. The column membrane was washed with 0.5 ml Buffer QG and 0.75 ml Buffer PE subsequently by 1 minute centrifugation steps at 13.000 rpm followed by another centrifugation step with the same parameters to dry the membrane. All flow-through of these steps was duly discarded. The DNA was then eluted with 50 µl DNase/RNase free water by a last centrifugation step (same parameters as above).

d) Restriction digestion

Next, both the vector and the insert were digested with the according restriction enzymes using the following reagents for 1 hour at 37° C.

Reagent	Amount
Insert or Plasmid scaffold	30 µl 2 µg
AgeI-HF EcoRI-HF or MfeI-HF 10x CutSmart™ Buffer DNase/RNase free water	20 U 20 U 4 µl to 40 µl

The digested products were again assorted by electrophoresis in 1,5% agarose gel and visualized under ultraviolet light to excise the gel region containing the correct products. The DNA was extracted from the gel as described before (in 2.2.2 c).

e) Ligation

The digested insert and plasmid were then ligated using the following reagents overnight at 16° C. The insert mass was estimated by applying the following formula:

$$\text{Insert Mass [ng]} = \frac{\text{5x plasmid mass [ng] * insert length [bp]}}{\text{plasmid length [bp]}}$$

Reagent	Amount
Insert	5-250 ng
Plasmid scaffold	50 ng
T4 DNA Ligase	1 µl
10x Ligase Buffer	1 µl
DNase/RNase free water	to 10 µl

f) Transformation

The ligation reaction mixture was then transformed into electrocompetent *E. coli* DH10B bacteria. For this, 1 µl of the reaction mix was transferred between the electrode plates of a Gene Pulser 0.1 cm cuvette (Bio-rad), 50 µl of the thawed bacteria suspension were added and the micropulser (Bio-rad) applied a 1.8 kV electromagnetic impulse. Immediately after electroporation, 250 µl of S.O.C. medium were added and the suspension incubated in a tube for 1 hour at 37° C and 350 rpm in a thermomixer (Eppendorf). A 50 – 150 µl suspension was plated on LB Kanamycin plates (33 µg/µl) and incubated overnight.

g) Mini culture and DNA purification

From the LB Kanamycin plate, clones were picked and inoculated in 6 ml of LB Kanamycin medium. They were then incubated for 8 - 12 hours at 37° C and 180 rpm. 2 ml of the cultures were separated in a new tube and centrifuged for 5 min at 13.000 rpm. The supernatant was discarded, the sediment resuspended in 250 µl buffer P1, 250 µl buffer P2 added and the reaction incubated for 5 min at room temperature. After supplementation of 300 µl buffer P3, the suspension was centrifuged for 10 min at 13.000 rpm and 4° C. The supernatant was transferred into new reaction tubes, 750 µl isopropanol added and the mix centrifuged again for 10 min at 13.000 rpm and 4° C. After having discarded the supernatant, 750 µl Ethanol 75% were added, centrifugation was repeated, and the supernatant was discarded again. The pellet containing the DNA was air-dried for 10 min and dissolved in 20 µl nuclease free water. 2 µg of the DNA was then sent for sequencing in a volume of 20 µl to MWG Eurofins Operon (Ebersberg).

h) Maxi culture and DNA purification

Appropriate clones identified by sequencing results were cultivated by inoculation of 100 µl in 200 ml of LB Kanamycin medium and incubation for 12-16 hours at 37° C and 180 rpm. DNA purification was performed using the EndoFree Plasmid Maxi Kit (Qiagen, Hilden) according to the attached manufacturer's instructions.

2.2.3 RNA isolation

For RNA extraction, the agent PeqGOLD Trifast™ was used. The latter is a solution of phenol and guanidine isothiocyanate which separates RNA, DNA and proteins into three phases after chloroform addition.

As standard procedure, cells were lysed in their dishes with 1 ml of peqGOLD Trifast™ for 3.5 cm dishes by mixing the cell suspension with a pipette. After dispersion, the reaction was incubated for 5 minutes at room temperature. After adding 200 µl chloroform, the containing tube was mixed with a vortex (Labinco L46) for 1 minute and incubated for 10 minutes at room temperature. The next step was a centrifugation for 10 minutes at 12.000 rpm and 4° C. The upper aqueous phase was transferred into a new tube and 500 µl isopropanol were added. The samples were incubated for 10 minutes on ice to allow precipitation of the RNA and centrifuged again for 10 minutes at 12.000 rpm and 4° C. The supernatant was discarded. The pellet was then dissolved and washed two times with 1 ml of 75% ethanol by mixing with a vortex for 10 seconds and centrifugation for 10 minutes at 12.000 rpm and 4° C. After discarding the supernatant and 10 minutes of air drying, the pellets were dissolved in 20 µl nuclease free water and frozen at -80° C. The RNA concentration was measured using a Nanodrop® ND-1000 spectrophotometer (peqLab, Erlangen).

2.2.4 Reverse transcription of mRNA

For better protection of the samples and reagents, both were thawed on ice. The following reagents were incubated in a new reaction tube for 10 minutes at 70° C for poly-A tail annealing of the oligo-dT primers:

Reagent	Amount
RNA	1 µg
Oligo-dT	2 µl
DNase/RNase free water	to 11 µl

A master mix was created with the following ingredients:

Reagent	Amount
5X first-strand buffer	4 µl
0.1 M DTT	2 µl
dNTP (10mM)	1 µl
RNase Inhibitor	0.1 µl
SuperScript™ II RT	1 µl
DNase/RNase free water	0.9 µl

9 µl of this master mix were added to the RNA reagent mix. Next, the reagents were incubated for 1 hour at 42° C, for 10 minutes at 70° C and finally stored on ice. The cDNA concentration was adjusted to 10 ng/µl by diluting it with nuclease free water.

2.2.5 Quantitative real time PCR of reversely transcribed mRNA

For quantification of the reversely transcribed mRNA we used quantitative real time PCR with the FastStart Universal SYBR Green Master (Rox) and a StepOne Plus instrument (Applied Biosystems, New Jersey). SYBR green intercalates into double-stranded DNA, hence emitting light as a fluorescent dye. Progressing duplication during PCR and light emission is detected by the instrument, which records an intensity curve over the reaction and normalizes this to the included reference fluorophore. By analyzing this curve, the instrument identifies the begin of exponential growth, which marks the cycle-threshold-value (C_t), informing about the initial quantity of the investigated mRNA. Triplicates of each sample were applied for C_t value calculation. This value is normalized to a reference mRNA in the cell, usually a housekeeping gene, in order to take into account different RNA extraction and cell qualities ($\Delta\Delta$-C_t method). For this purpose, GAPDH mRNA were used. A RNA-free triplicate and a Taq polymerase-free triplicate served as controls.

All reagents were thawed and kept on ice during preparation of a master mix. The following reagents were mixed:

Reagent	Amount
FastStart Universal SYBR Green Master (Rox)	6.25 µl
Forward primer (20 pmol/µl)	0.25 µl
Reverse primer (20 pmol/µl)	0.25 µl
cDNA	10 ng
DNase/RNase free water	to 12.5 µl

The following thermal cycling program was used:

Stage	Step	Duration	Temperature	Cycles
1	Polymerase Activation	10 min	95° C	1
2	Denaturation	15 s	95° C	40
	Annealing	30 s	58° C	
	Extension	15 s	65° C	
3	Holding stage	1 min	65° C	1
4	Melting Curve (primer specificity testing)	117 min	60-95° C; 0.3°C increase/min	1

2.2.6 Reverse transcription of microRNA

For reverse transcription and quantitative real time PCR of microRNA, the miRCURY LNA™ Universal RT microRNA PCR kit was used. All reagents were gently thawed on ice. The isolated RNA was adjusted to a concentration of 5 ng/µl using nuclease free water.

A master mix was created with the following ingredients:

Reagent	Amount
5x Reaction buffer	2 µl
DNase/RNase free water	5 µl
Enzyme mix	1 µl

8 µl of this master mix were placed in new tubes and 2 µl of the RNA samples were added. Then the reagents were incubated for 1 hour at 42° C, for 5 minutes at 95° C and cooled down to 4° C.

2.2.7 Quantitative real time PCR of microRNA

The cDNA was diluted on a 1:80 basis in nuclease free water. A master mix was created with the following ingredients:

Reagent	Amount
FastStart Universal SYBR Green Master (Rox) PCR primer set	5 µl 1 µl

6 µl of this master mix were placed in qPCR plate wells and 4 µl of the diluted cDNA were added, the plate sealed with an optical sealing and placed in the PCR instrument.

The following thermal cycling program was used:

Stage	Step	Duration	Temperature	Cycles
1	Polymerase Activation/Denaturation	10 min	95° C	1
2	Denaturation	15 s	95° C	40
	Annealing/Extension	60 s	60° C	

2.2.8 Culture of HEK293 cells

HEK293 cells were applied for the double fluorescent reporter studies. For this, HEK293 cells were cultured in a medium containing:

- Dulbecco's Modified Eagle Medium (DMEM)
- 10% fetal bovine serum (FBS)
- 1% L-glutamine
- 1% Penicillin (10000U/ml)/Streptomycin (100mg/ml)

They were incubated at 37° C in a 5% CO_2 humid atmosphere. Cells were split every third to fourth day to maintain monolayer cultures. Splitting was carried out via one washing step with Dulbecco's phosphate buffered saline (DPBS), treatment with trypsin-EDTA to degrade adhesion proteins and dilution in new medium and dishes.

2.2.9 Isolation of neonatal primary cells

The following cell preparation was performed by qualified technical assistants. Newborn Sprague-Dawley rats (1-2 days postnatal) were separated. Whole hearts

were excised after euthanasia and immediately incubated in Hank's balanced salt solution (HBSS, HEPES-buffered, Ca^{2+} and bicarbonate-free). The atria were removed and the rest of the cardiac tissue was minced and incubated in a digestion solution containing trypsin and DNase which was constantly and slowly stirred. After dissolution of tissue connections, the cells were transferred into fetal bovine serum and filtered through a 40 µm cell strainer. The flow-through was incubated for 1 hour at 37° C in an atmosphere containing 1% CO_2 in uncoated dishes to split the faster adhering fibroblasts from the cardiomyocytes, which remain in the supernatant. This supernatant was added to a medium containing DMEM, 1% FBS, vitamin B_{12}, BrdU and $NaHCO_3$. The resulting cell suspension containing the cardiac myocytes was used for further experiments and culturing. Cell density was counted by adding 50 µl of Trypan blue to 50 µl of the cell suspension and measuring the cell number in 10 µl of this mix with a Countess cell counter (Thermo Fisher Scientific, Waltham, USA). The aforementioned attached cardiac fibroblasts were washed once with DPBS. They were cultured in a medium containing DMEM, 1% FCS, vitamin B_{12} and $NaHCO_3$.

2.2.10 NRCM hypertrophy assay

a) Culture & transfection

The NRCM suspension of 2.2.9 were seeded in a 96-well IBIDI plate in a density of 50.000 cells/well in a 1% NRCM medium. Cells were incubated for 24 hours at 37° C and 1% CO_2.

The transfection of microRNAs was conducted with Lipofectamine™ 2000.

For this, 2 master mixes named A and B with the following ingredients per well were created:

Reagent	Amount
Mix A: - Lipofectamine™ 2000 - Opti-MEM	 0.25 µl 24.75 µl
Mix B: - microRNA/antimiR - Opti-MEM	 0.25 µl (50 nM) to 25 µl

For the mock control group, mix B consists of 25 µl Opti-MEM without microRNA/antimiR. Both mixes were incubated for 5 min at room temperature. After mixing A with B the resulting mix was incubated for another 20 min at room temperature. During the incubation time, the NRCM 96-well plate was washed with 1% NRCM medium without antibiotics and 50 µl of this medium were added. 50 µl of the transfection mix were added to each well to achieve a final concentration of 50 nM as recommended. The cells were incubated with this 100 µl transfection solution for 6 hours at 37° C in an atmosphere containing 1% CO_2. The medium was changed to 200 µl of 0.1% NRCM medium with antibiotics and incubated for 24 hours at the same conditions afterwards.

Cells were stimulated over 48 hours with a 50 µM Phenylephrine in a 0.1% NRCM medium. Cells receiving no PE stimulation were incubated in 200 µl of 0.1% NRCM medium.

b) Staining & Microscopy

Cells were fixed by incubation with 100 µl 4% Paraformaldehyde for 5 minutes. They were washed thrice with 200 µl PBS and permeabilized with 100 µl of 0.2% Triton™ X-100. The cells were then incubated with the first antibody against α-actinin (1:1000 in 100 µl PBS) for 30 min at 37° C. After a washing step, the cells were incubated with a secondary antibody, a Alexa488-conjugated goat anti-mouse IgG (1:200), and DAPI (1:100) in 100 µl of PBS. Again, the plate was washed three times, 150 µl of 50% glycerol were added and the plate sealed with an aluminum seal. Until automated microscopy, the plates were stored at 4° C in darkness.

The automated microscopy was able to identify cardiac myocytes by capturing cell nuclei stained with DAPI surrounded by α-actinin, thus providing information about the cell size by measuring the fluorescent area (Jentzsch, Leierseder et al. 2012).
The equipment consisted of a microscope with a 10x objective, an AxioObserver.Z1 (Zeiss, Jena, Germany), a motorized scanning stage (130 × 85; Märzhäuser, Wetzlar, Germany), a Lumen200 fluorescence illumination system (Prior, Cambridge, UK) and a Retiga-4000DC CCD camera (QImaging, Surrey, Canada).

The software MetaMorph Basic journals/macro functions were programmed by the colleagues listed in the publication of Jentzsch, Leierseder et al. They programmed one master journal built upon three sub journals. The first sub journal regulated the mechanical operations, e.g. positioning, focusing, taking four photos per well in two different fluorescence channels. The second sub journal merged the different fluorescence channel photos to one overlay image. The third sub journal used multiple Metamorph plugins to analyze the acquired images and create a table containing all necessary values.

c) siRNA rescue hypertrophy assay

As a variant of the hypertrophy assay described above, a siRNA rescue hypertrophy assay was carried out. As this assay is far more challenging for the damageable NRCMs, the seeded cell number was 50000-80000/well, depending on the viability. Seeding and culture were performed identically. On the first day after seeding, siRNA was transfected instead of microRNA/antimiR. The antimiR was transfected 24 hours later. Another 48 hours later, the cells were stimulated with phenylephrine as described above (2.2.10 a) and 48 hours later the cells were fixed.

2.2.11 DF-reporter assay

For the double fluorescent reporter assay, which was constructed in 2.2.2, the freshly split HEK293 cells of 2.2.8 were cultured. 30.000 cells/well were seeded on a 96-well IBIDI plate. 24 hours later, the transfection of 200 ng of the reporter and 50nM of microRNA was conducted following the protocol described above (2.2.10a).
48 hours later, the cells were fixed by incubation with 100 µl of 4% Paraformaldehyde for 5 minutes. They were washed thrice with 200 µl PBS, 150 µl of 50% glycerol were added and the plates sealed with an aluminum seal. They were stored at 4° C in darkness until automated microscopy.
The automated microscopy captured the green fluorescence and the red fluorescence emitted by the proteins transcribed of the reporter with the same hardware as described in 2.2.10b. Due to this fact, it was not only possible to identify the presence of fluorescence and define cells and their borders, but also to measure the intensity of both emissions of every single cell. This information was processed to quantify the ratio

of both fluorescence emissions in each cell and show the connection to transfection efficiency of the reporter and microRNA.

2.2.12 Statistics

All statistical analysis in this study was performed with the software Graph Pad Prism (5.0b). Two groups were compared using the unpaired *student's t-test*. If the sample number did not suffice to test for normality, a non-parametric test (Mann-Whitney U-test) was used. Differences were called significant if $p < 0.05$, and were represented by an asterisk (*). If $p < 0.01$, the representation was **. If $p < 0.01$, it was ***.

3 Results

3.1 miR-365 expression *in vitro*

To characterize the endogenous level and role of miR-365 in the cardiac cells under hypertrophic conditions, the expression level of miR-365 *in vitro* was measured. In neonatal rat cardiac myocytes (NRCM), a slight but not significant increase of miR-365 expression was detected under phenylephrine (PE) stimulation. In neonatal cardiac fibroblasts (NRCF), the expression of miR-365 was upregulated after both PE and Angiotensin II (AngII) treatment (Figure 7). This suggests a regulation of expression under hypertrophic conditions in cardiac myocytes and in particular in cardiac fibroblasts.

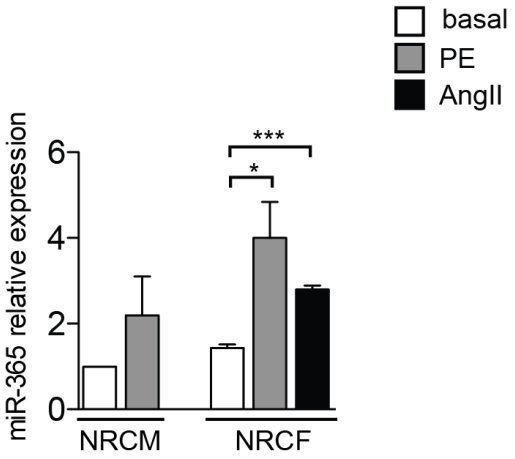

Figure 7: Expression of miR-365 in NRCM and NRCF. Expression of miR-365. Expression of miR-365 in NRCM and NRCF under basal conditions and under stimulation with PE or Ang II (n=3); an unpaired *student's t-test* was used to calculate the statistical differences denoted; *P<0.05, ***P<0.001

3.2 microRNA-365 hypertrophic effect *in vitro*

In order to confirm the reported prohypertrophic effect of miR-365 *in vitro*, the effect of miR-365 in cultured NRCM under basal conditions and under adrenergic stimulation with PE was investigated.

Transfection of miR-365 resulted in a significant increase in CM cell size under basal conditions compared to cells transfected with the control microRNA. Reciprocally, the increase of cell size by PE stimulation was significantly reduced by transfection of

antimiR-365 compared to the cells transfected with the control anti-microRNA (Figure 8). These results confirm the strong prohypertrophic effect of miR-365, which exceeds the effect of single PE stimulation. Reversely, antimiR-365 blocked the prohypertrophic stimulus of PE treatment.

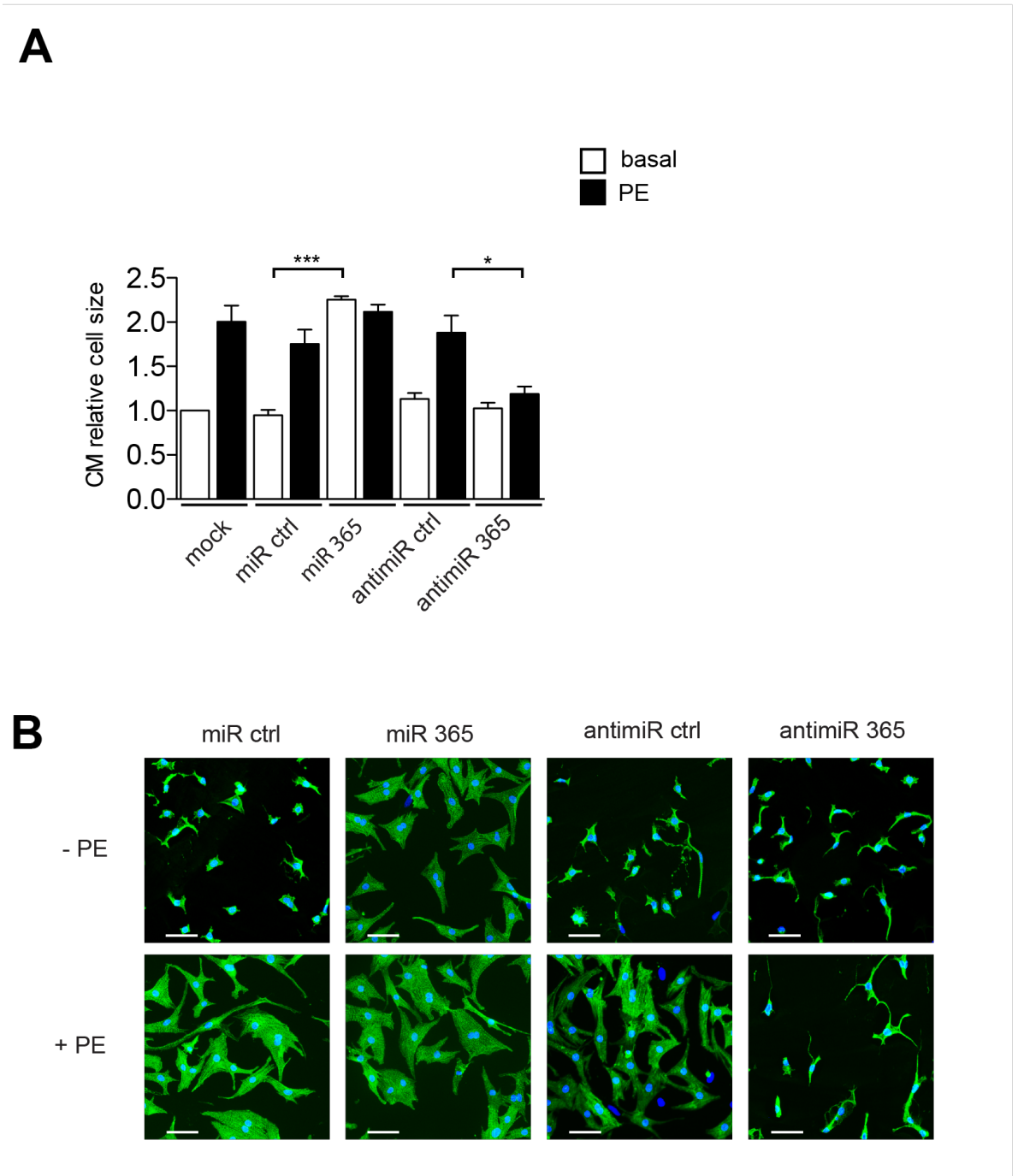

Figure 8: miR-365 has a hypertrophic effect on NRCM. (A) Comparison of cell size of NRCM *in vitro* under basal conditions and after stimulation; Cells were transfected with the following solutions: mock, miR-365 antimiR-365 and their respective controls (n=3). **(B)** Representative microscopy images of NRCM transfected with either miR-365, antimiR-365 or their respective controls in the presence or absence of PE; Scale bar: 50 µm; an unpaired *student's t-test* was used to calculate the statistical differences denoted; *P<0.05, ***P<0.001

3.3 miR-365 target evaluation

After confirmation of the prohypertrophic effect of miR-365, investigation of the mechanistic background and potentially regulated target genes responsible for this effect was started. Consequently, a miR-365 target screening was performed. Validated targets of miR-365 in human skeletal muscle by a collaborative group (Dmitriev, Stankevicins et al. 2013) were analyzed for highly conserved binding sites for miR-365 in human, mouse and rat and a sufficient mRNA target abundance in cardiac myocytes. 5 genes met these criteria. These potential targets were selected if there was a reported relation to cardiac hypertrophy regulation. Finally, the remaining 4 genes were tested for mRNA expression regulation by miR-365. As a result of this screening, one of the most promising target candidates of miR-365, *Cnot6l,* was selected.

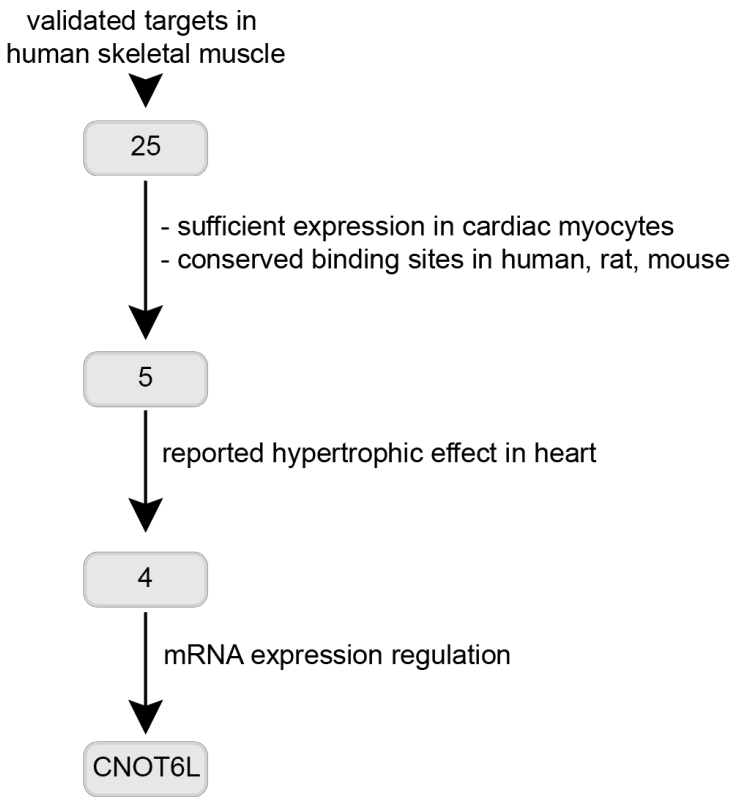

Figure 9: miR-365 target screening. 25 validated targets of miR-365 in human skeletal muscle were analyzed with bioinformatics under multiple criteria and tested for a sufficient mRNA expression regulation.

Cnot6l is a highly conserved gene as a subunit of the CCR4-NOT complex. The latter is abundant in diverse organisms and cells from yeast to human. It exhibits two binding sites for miR-365 in its 3'UTR (and another in its open reading frame (ORF)) that are conserved over numerous species including human, mouse, rat and pig (Figure 10).

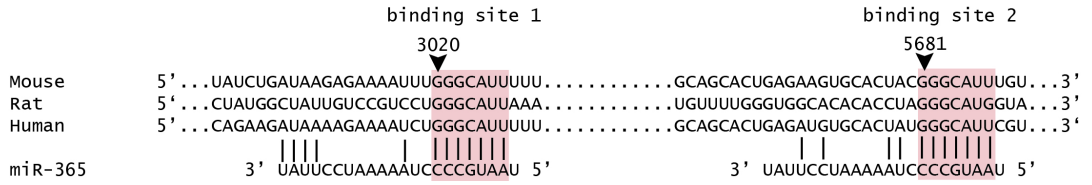

Figure 10: binding sites for miR-365 in Cnot6l mRNA are highly conserved. Alignment of mouse (NM_001285511.1), rat (NM_001108355.1) and human (NM_001286790.1) mRNA binding sites for the miR-365 seed sequence.

3.3.1 miR-365 *Cnot6l* regulation

In order to find confirmation for the regulation of *Cnot6l* by miR-365, first a quantitative real time PCR (qPCR) on RNA extracted from NRCM transfected with either miR-365 mimics or an antimiR-365 was conducted.

In NRCM, miR-365 overexpression induced a significant reduction of *Cnot6l* mRNA level, reciprocally *Cnot6l* mRNA levels were significantly increased after miR-365 inhibition (Figure 11).

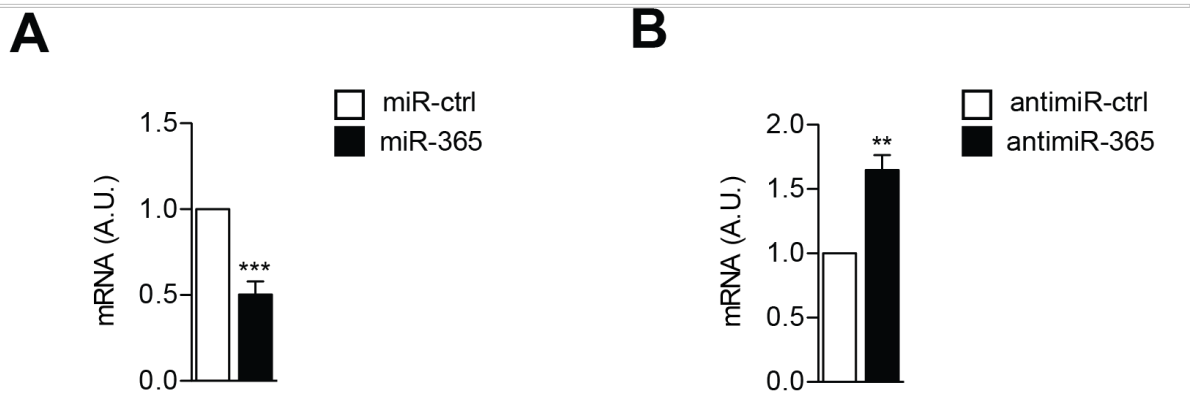

Figure 11: *Cnot6l* mRNA expression after transfection of miR-365 or antimiR-365. (A) *Cnot6l* mRNA expression in NRCM after transfection of miR-365; **(B)** *Cnot6l* mRNA expression in NRCM after transfection of antimiR-365 (n=7-8); an unpaired *student's t-test* was used to calculate the statistical differences denoted; **P<0.01, ***P<0.001

To show the direct interaction between *Cnot6l* mRNA and miR-365, a double fluorescent reporter assay on HEK cells with DF-*Cnot6l* and miR-365 mimics was performed.

Briefly summarized, the DF-*Cnot6l* reporter contains a red and a green fluorescent protein gene. While the RFP is used for normalization purposes, the region of the *Cnot6l* 3'-UTR, which exhibits the two binding sites for miR-365, is attached to the GFP gene. MiR-365 binds to this 3' insert of the GFP mRNA by targeting these binding sites and prevents its translation. As a result, an increased miR-365 level leads to a reduced GFP to RFP emission-ratio (Figure 12B).

In HEK cells, the GFP to RFP emission-ratio was significantly reduced after transfection of miR-365 mimics compared to miR control, which visualizes the direct interaction of miR-365 with the 3' insert (Figure 12C).

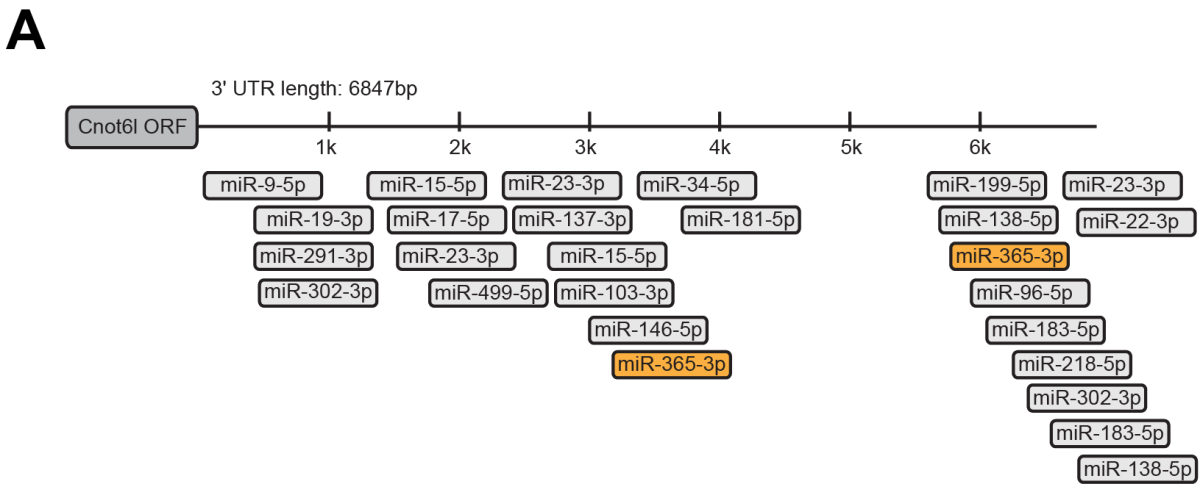

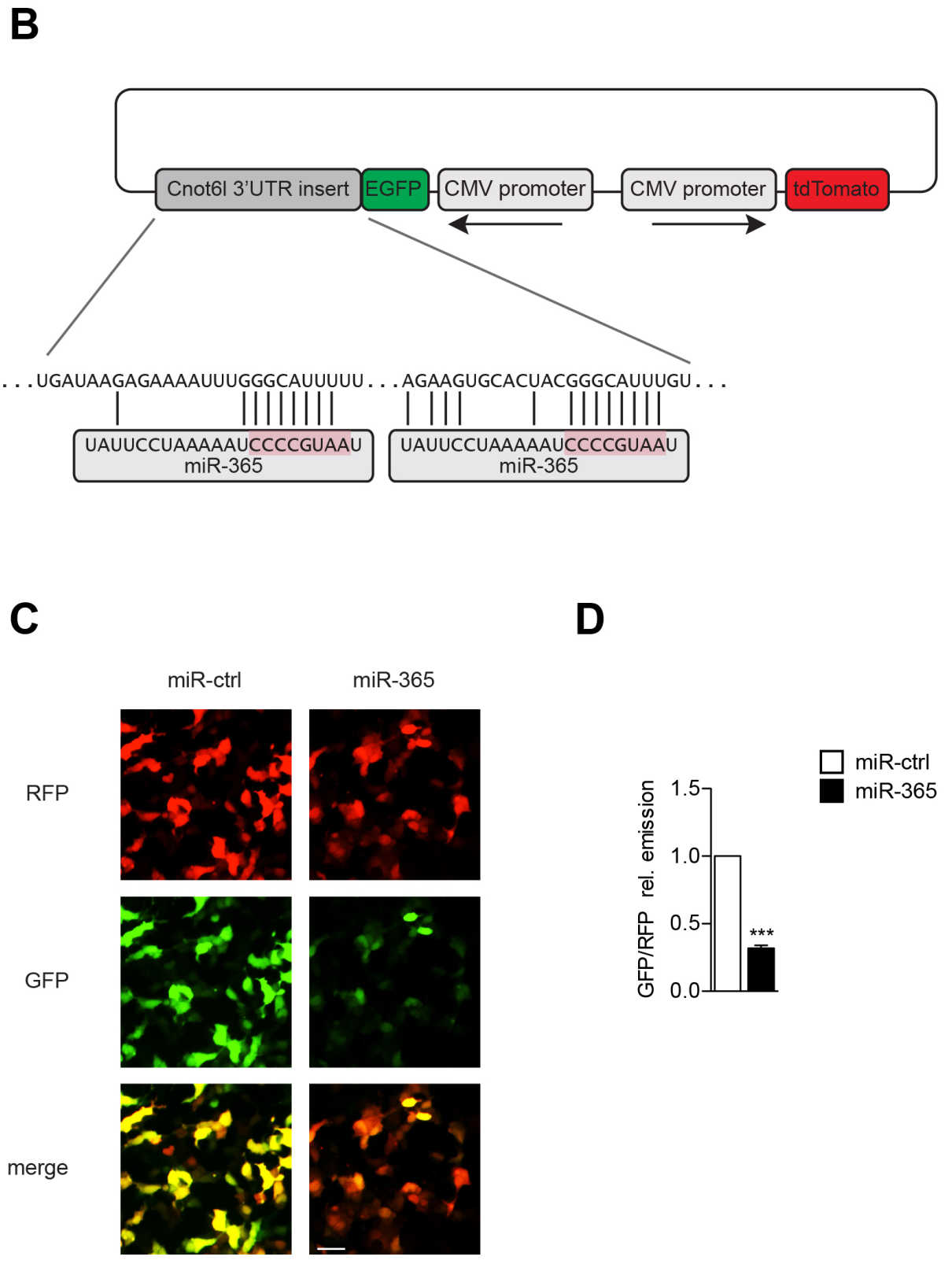

Figure 12: miR-365 directly regulates Cnot6l. (A) Scheme of *Cnot6l* 3'UTR and broadly conserved microRNA binding sites in vertebrates including the location of binding sites for miR-365; **(B)** Illustration of the double fluorescent reporter including the insert with the binding sites for miR-365; **(C)** Representative microscopy images of HEK293 cells transfected with either miR-365 or control; scale bar: 50 µm; **(D)** GFP to RFP ratio of DF- *Cnot6l* reporter in HEK cells after transfection of miR-365 or control (n=4); an unpaired *student's t-test* was used to calculate the statistical differences denoted. ***P<0.001

Taken together, these results indicate the direct regulation of *Cnot6l* by miR-365 leading to a significant change of its mRNA level by degradation in cardiac myocytes.

3.3.2 miR-365 *Cnot6l* siRNA rescue

In summary, MiR-365 has a prohypertrophic effect on cardiac myocytes and antimiR-365 blocks hypertrophic reactions (e.g. to PE). It is shown above that *Cnot6l* is a direct target of miR-365. As reported by a variety of studies, other subunits of the CCR4-NOT complex regulate cardiac hypertrophy (Neely, Kuba et al. 2010, Zhou, Liu et al. 2017). Therefore, it was assumed that this hypertrophic effect is achieved by suppression of this target, so the antihypertrophic effect of antimiR-365 is reached by a derepression of *Cnot6l*.

As a consequence of that, transfection of a siRNA targeting *Cnot6l* should have a similar effect as miR-365 and should reverse the antimiR-365 anti- hypertrophic effect (Figure 13B). These effects are visualized in the siRNA rescue trial below.

Figure 13C shows tendencies of these effects. Mean cell sizes of NRCM transfected with *siCnot6l* are increased in all groups, even though the differences achieved by this rescue were not significant.

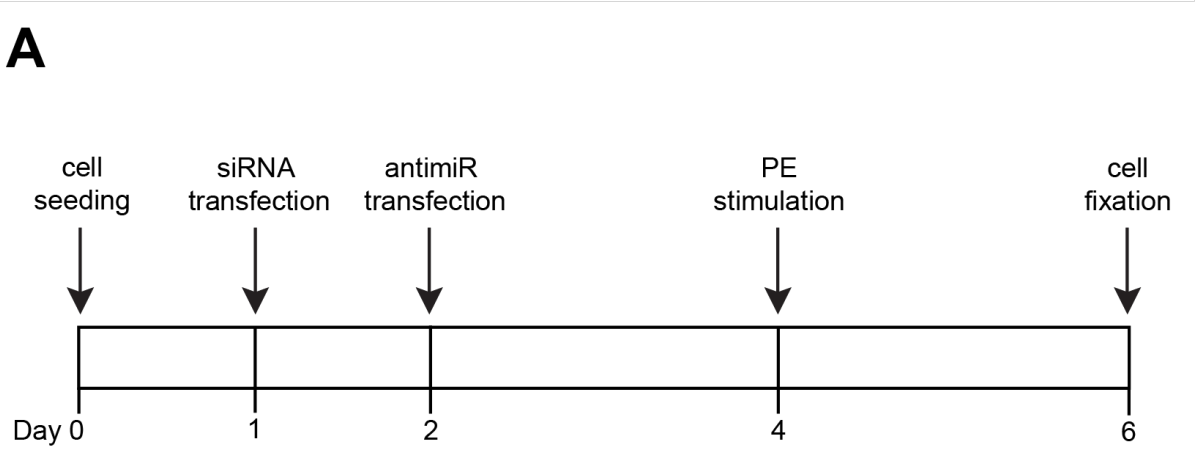

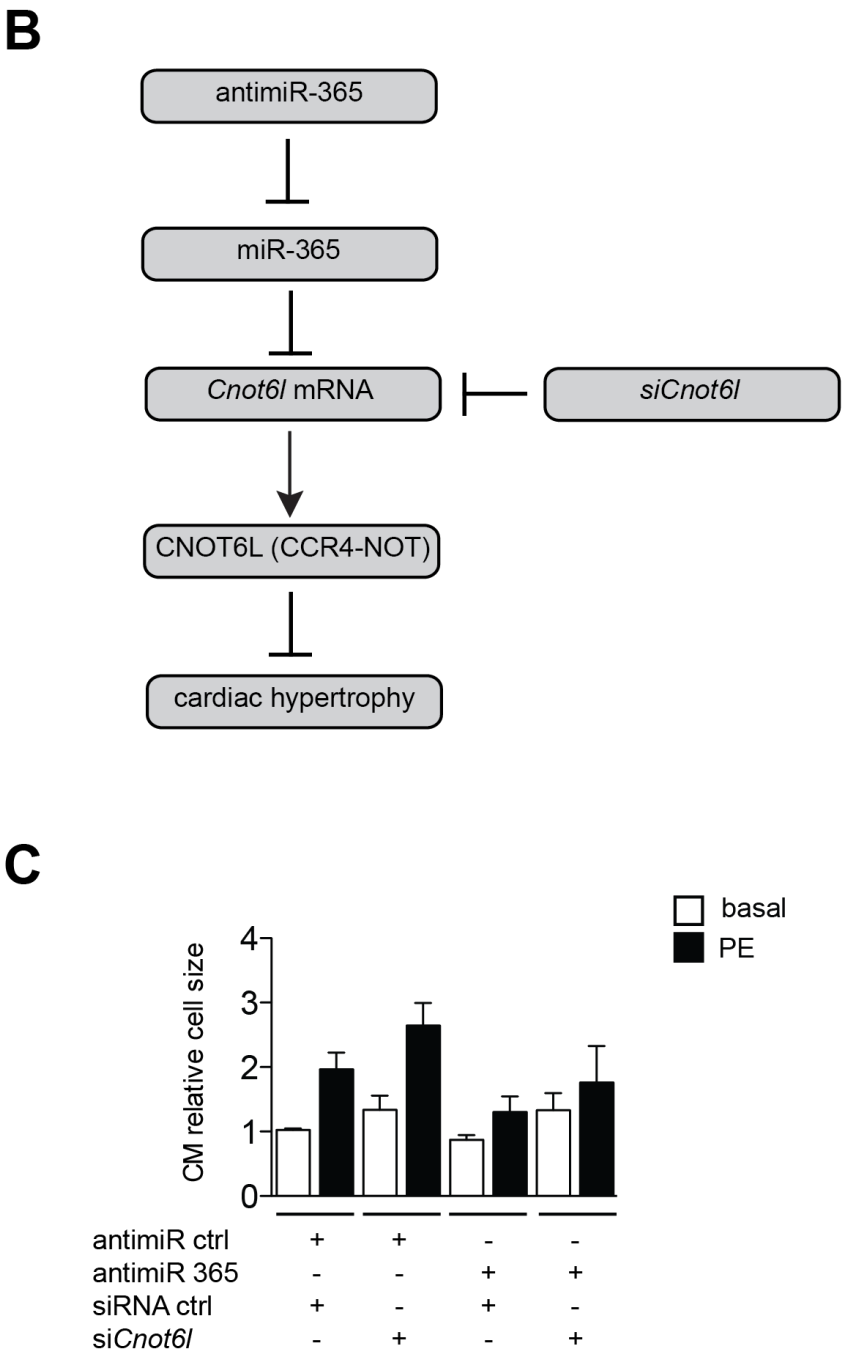

Figure 13: siRNA rescue hypertrophy assay. (A) Time table of siRNA rescue hypertrophy assay; **(B)** Scheme illustrating the mechanism of siRNA rescue; **(C)** Graph of the siRNA rescue study: antimiR-365 blocked the hypertrophic stimulus of PE, simultaneous si*Cnot6l* transfection tended to a reduction of this blockade (n=4).

3.4 miR-29 target evaluation

After confirming the observed hypertrophic effect of miR-29 which was seen in the phenotypic screening, the regulated targets of the miR-29 family which led to the

observed cell changes were identified. A bioinformatic approach was used to find high potential targets and observed an enrichment of Wnt pathway members.
As miR-29 is described to manipulate Wnt signaling in other tissues and Wnt signaling is activated in pathologic cardiac conditions, it was verified that miR-29 directly regulates Wnt signaling in cardiac cells, too.
In this study, the regulation of *Hbp1*, *Glis2* and *Ctnnbip1* by miR-29 was investigated.

3.4.1 miR-29 *Ctnnbip1* regulation

The catenin beta interacting protein 1 (Ctnnbip1), also referred to as inhibitor of beta-catenin and Tcf-4 (ICAT), exhibits a conserved binding site in its 3'UTR (Figure 14A and B).
First, qPCR on NRCM after transfection of miR-29a to investigate mRNA expression changes of *Ctnnbip1* was performed. A significant reduction of expression after transfection of miR-29 was found (Figure 14D).
Second, miR-29a or a control microRNA and a double fluorescent reporter with the *Ctnnbip1* 3'UTR region exhibiting the miR-29 binding site into HEK-293 cells were transfected. A significant reduction of the green to red fluorescence emission-ratio after transfection of miR-29a, showing a direct interaction of miR-29a with the said insert was observed (Figure 14C and E).

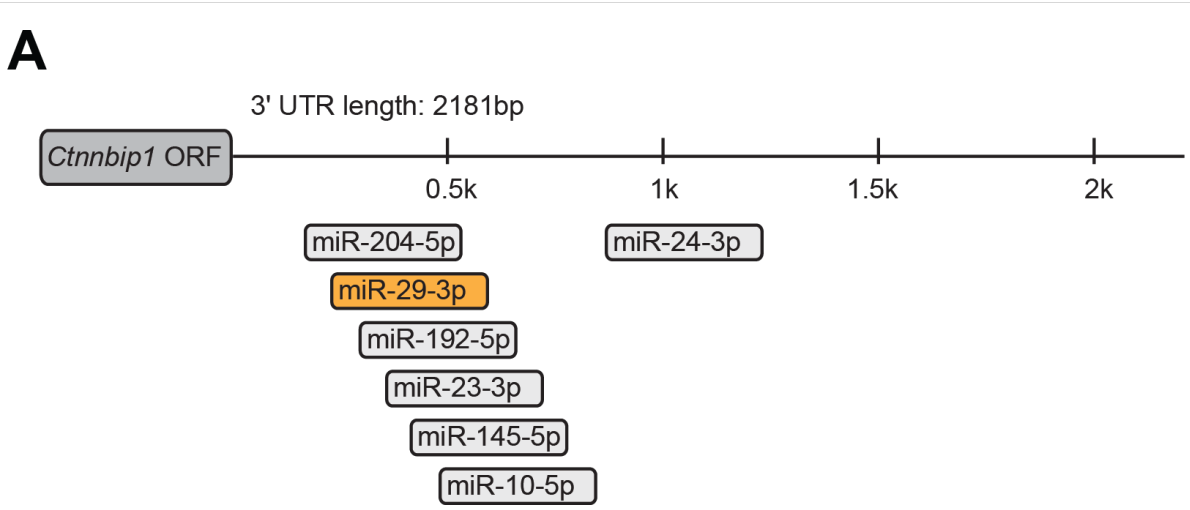

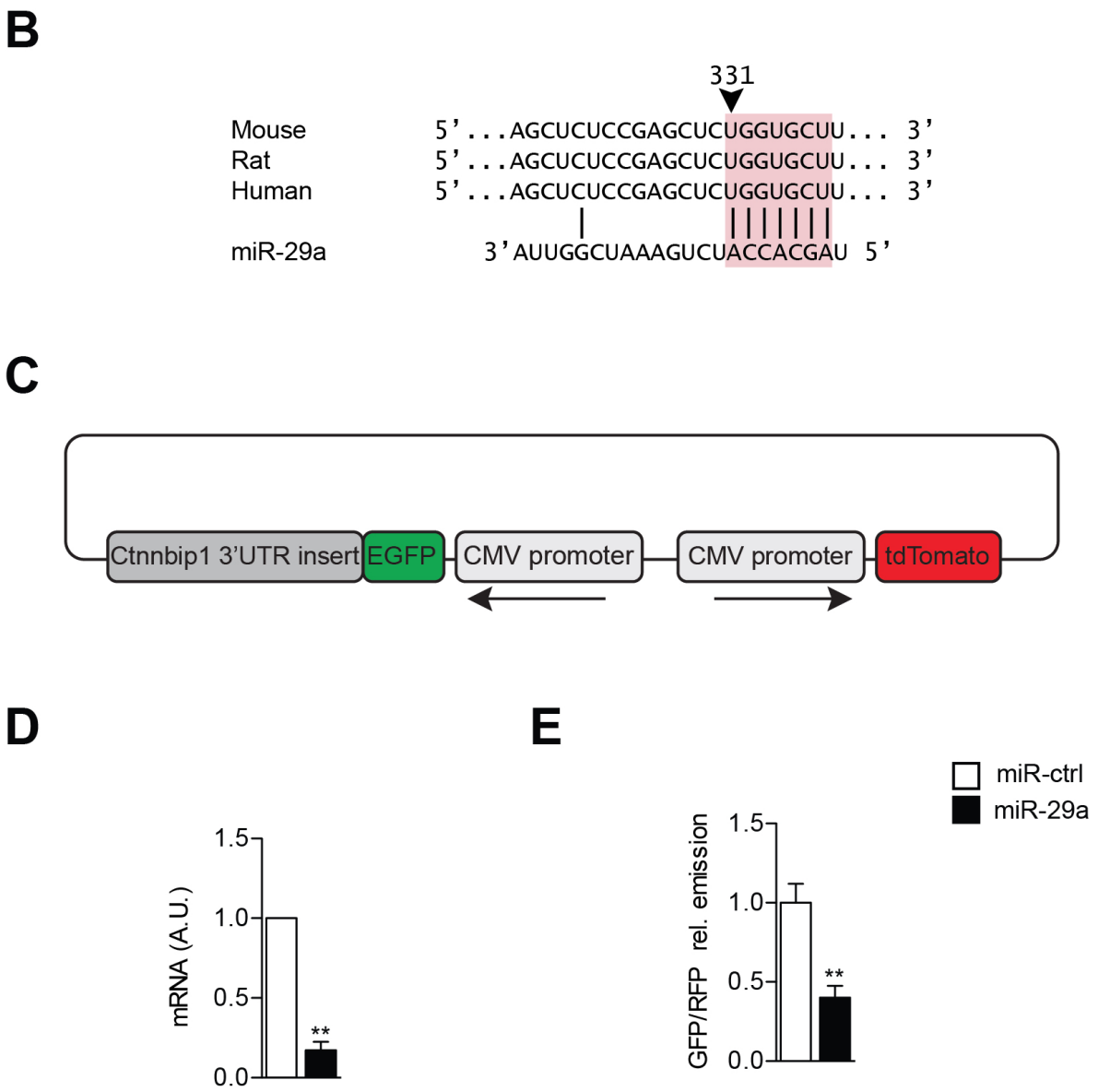

Figure 14: miR-29 directly regulates *Ctnnbip1*. (A) Scheme of *Ctnnbip1* 3'UTR and broadly conserved microRNA binding sites in vertebrates including the location of the binding site for miR-29; **(B)** Ctnnbip1 3'UTR binding site alignment of mouse (NM_023465.4), rat (NM_001173388.1) and human (NM_001012329.1) to miR-29a; **(C)** Illustration of the double fluorescent reporter including the insert with the binding site for miR-29; **(D)** Target mRNA expression in NRCM after transfection of miR-29a compared to their controls (n=3); **(E)** GFP to RFP emission-ratio after transfection of miR-29 or its control and double fluorescent reporter in HEK293 cells (n≥3); an unpaired *student's t-test* was used to calculate the statistical differences denoted; **P<0.01

3.4.2 miR-29 *Glis2* regulation

The Kruppel-Like Zinc Finger Protein GLIS2 also comprises one miR-29 binding site in its 3'UTR (Figure 15A and B).

The mRNA expression changes of *Glis2* in NRCM after transfection of miR-29a were measured, which showed a significant reduction of expression (Figure 15D).

In addition for this potential target, a double fluorescent reporter with the *Glis2* 3'UTR region exhibiting the miR-29 binding site and miR-29a or a control microRNA was transfected into HEK-293 cells. A significant reduction of the green to red fluorescence emission-ratio after transfection of miR-29a was measured, demonstrating a direct interaction of miR-29a with the insert (Figure 15C and E).

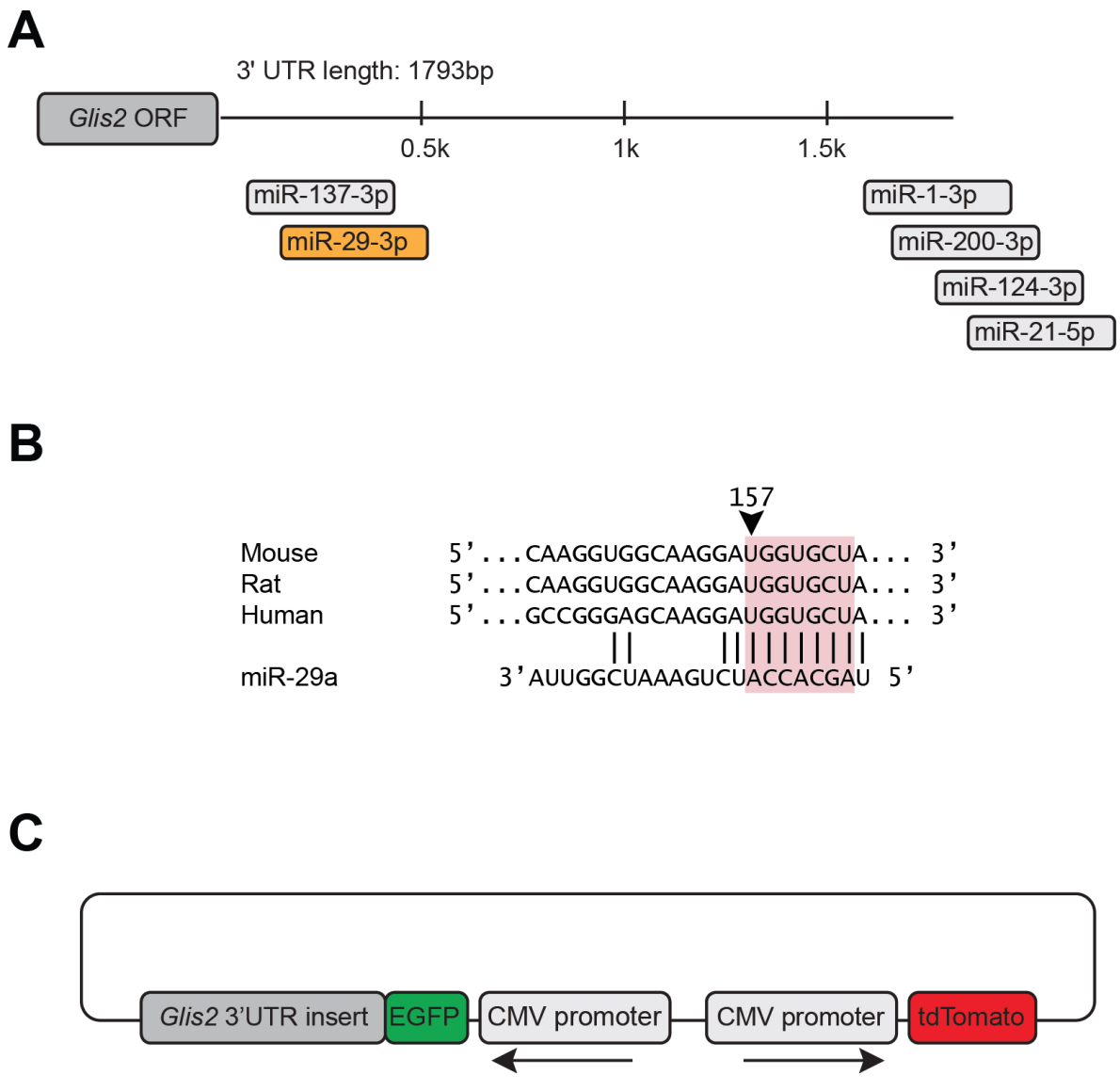

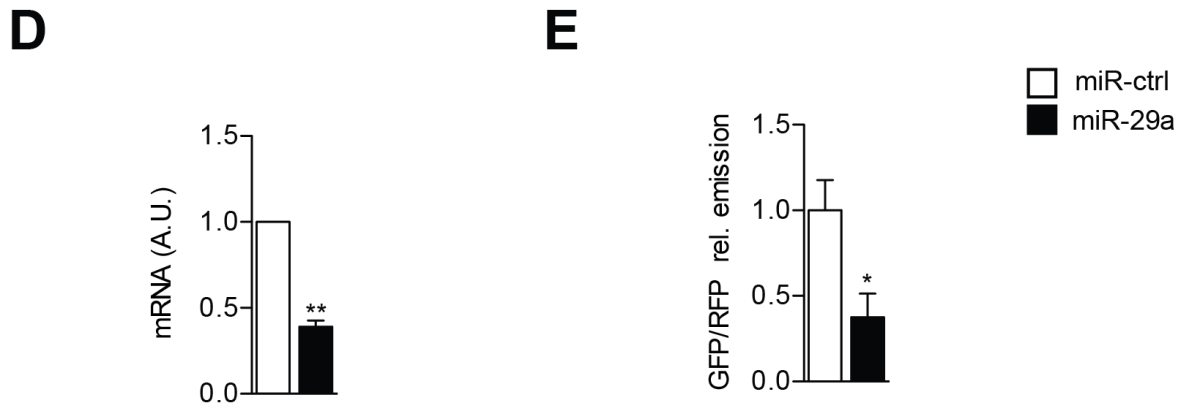

Figure 15: miR-29 directly regulates *Glis2*. (A) Scheme of *Glis2* 3'UTR and broadly conserved microRNA binding sites in vertebrates including the location of the binding site for miR-29; **(B)** Glis2 3'UTR binding site alignment of mouse (NM_031184.3), rat (NM_001106978.1) and human (NM_001318918.1) to miR-29a; **(C)** Illustration of the double fluorescent reporter including the insert with the binding site for miR-29; **(D)** Target mRNA expression in NRCM after transfection of miR-29a or antimiR-29 compared to their controls (n=3); **(E)** GFP to RFP emission-ratio after transfection of miR-29 or control and the double fluorescent reporter in HEK293 cells (n≥3); an unpaired *student's t-test* was used to calculate the statistical differences denoted; *P<0.05, **P<0.01

3.4.3 miR-29 *Hbp1* regulation

The HMG-box transcription factor 1 (HBP1) 3'UTR possesses two conserved miR-29 binding sites (Figure 16A and B).

To show mRNA alterations in expression of *HBP1*, a qPCR on NRCM after transfection of miR-29a was conducted, which showed a significant reduction of expression after transfection (Figure 16D).

To prove the direct interaction between miR-29 and the two binding sites, miR-29a or a control microRNA and a double fluorescent reporter with the *Hbp1* 3'UTR region, exhibiting the miR-29 binding sites into HEK-293 cells, were transfected, which a significant reduction of the green to red fluorescence emission-ratio after transfection of miR-29a (Figure 16C and E).

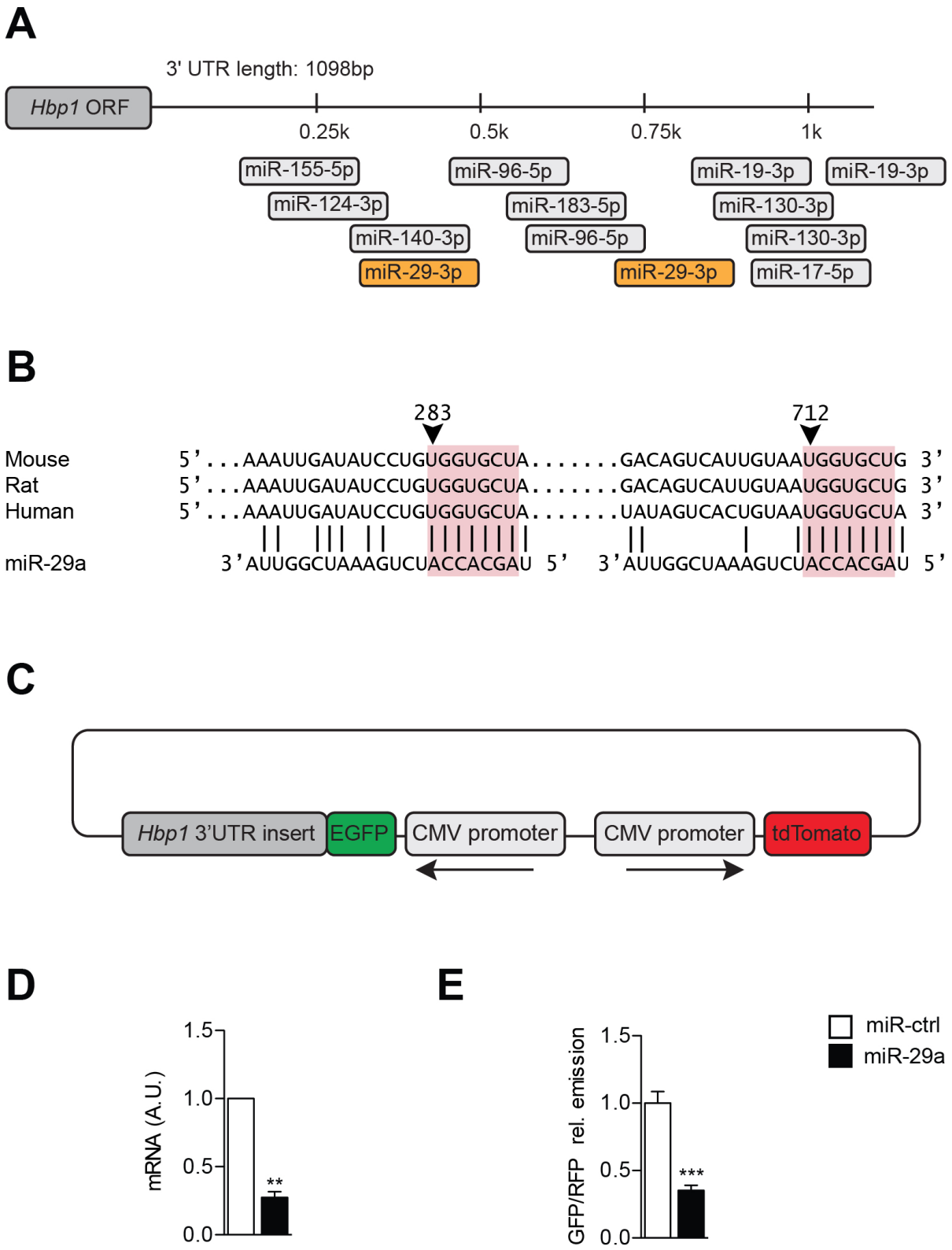

Figure 16: *Hbp1* is directly regulated by miR-29. (A) Scheme of *Hbp1* 3'UTR and broadly conserved microRNA binding sites in vertebrates including the location of the binding sites for miR-29; **(B)** Hbp1 3'UTR binding sites alignment of mouse (NM_153198.2), rat (NM_013221.2) and human (NM_012257.3) to miR-29a; **(C)** Illustration of the double fluorescent reporter including the insert with the binding sites for miR-29; **(D)** target mRNA expression in NRCM after transfection of miR-29a (n=3); **(E)** GFP to RFP emission-ratio after transfection of miR-29 or control and the double fluorescent reporter in HEK293 cells (n≥3); an unpaired *student's t-test* was used to calculate the statistical differences denoted; **P<0.01, ***P<0.001

4 Discussion

Since their first description in 1993, microRNAs have developed from a rarity observed in nematodes to a large category of RNA crucial for gene expression in animals as well as plants, in numerous cell types for embryology, differentiation, maintenance, health and disease.

Contributing to this process of research, this study investigates two different microRNAs and their regulation of cardiac remodeling.

4.1 miR-365, Cnot6l and cardiac hypertrophy

4.1.1 miR-365 in cardiac hypertrophy

First, the prohypertrophic effect of miR-365 reported in a phenotypic screening (Jentzsch, Leierseder et al. 2012) was confirmed in an *in vitro* hypertrophy assay. Having executed these, a more than two-fold increase in cell size outreaching the measured effect of cells treated with PE was observed.

Another recently published study also reported on the prohypertrophic effect of miR-365 (Wu, Wang et al. 2017). This study showed that miR-365 inhibits autophagy by targeting the S-phase kinase-associated protein 2 (Skp2), a cell cycle regulator. Moreover, miR-365 upregulations were found *in vitro* by Angiotensin II treatment and *in vivo* after TAC operation in murine cardiac myocytes. This is in line with the observations *in vitro* concerning miR-365 expression in NRCM and NRCF after stimulation of this study (Figure 7).

Connecting these findings to this study, miR-365 seems to regulate the turnover of gene products on the RNA and on the protein level (see 4.1.2). These regulation mechanisms, both influencing cellular homeostasis, certainly could have an impact on neoplastic processes, that are constituting the main field of recent miR-365 research (see 1.4), too. Furthermore, both targets are reported to have oncogenic effects (Carrano and Pagano 2001, Bashir, Dorrello et al. 2004) that are to be discussed in further detail for CNOT6L in the next chapter.

4.1.2 *Cnot6l*, the CCR4-NOT complex and cardiac hypertrophy

In this study, it is explained both that miR-365 regulates *Cnot6l* directly as well as that their manipulation can lead to cardiomyocyte hypertrophy.

CNOT6L is part of the deadenylase subunits of the mammalian carbon catabolite repression 4 (CCR4)-negative on TATA-less (NOT) complex. It exhibits catalytic capacity and is a member of the exonuclease/endonuclease/phosphatase (EEP) family. Initially, the CCR4-NOT complex was investigated in yeast (Collart 2003). Later, it was found to be one of the most dominant enzyme complexes for cytoplasmatic degradation of RNA with poly(A) residues following the deadenylation initiation of PAN2-PAN3 (Yamashita, Chang et al. 2005, Wang, Morita et al. 2010). The deadenylase subunits are built of two parts containing CNOT6 or CNOT6L and CNOT7 or CNOT8 (Figure 17A).

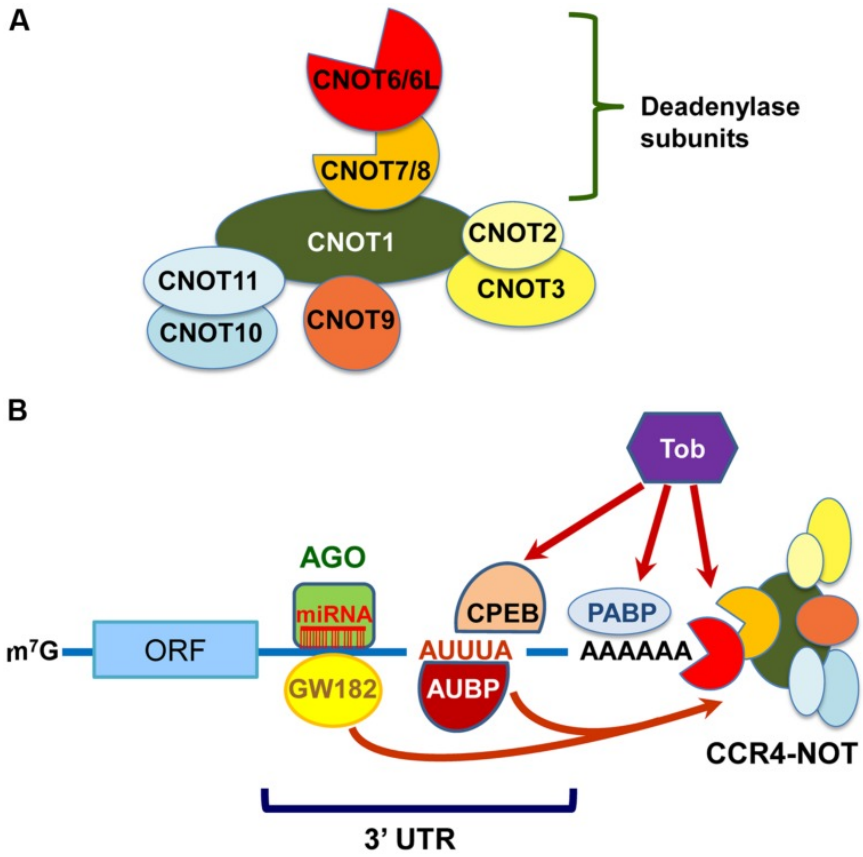

Figure 17: The mammalian carbon catabolite repression 4 (CCR4) – negative on TATA-less (NOT) complex exerts deadenylase activities guided by RNA-binding proteins, miRISC and Tob (Shirai, Suzuki et al. 2014). (A) Structure of the CCR4-NOT complex and its subunits. **(B)** The CCR4-NOT complex in context of recruiting molecules.

Synonyms for the mammalian CNOT6 and CNOT6L are CCR4a and CCR4b.
The CCR4-NOT complex can be recruited by the miRISC through GW182 if it contains CNOT7 and/or CNOT6L, depending on sequences and helper proteins, e.g. PABP (Figure 17B) (Fabian, Mathonnet et al. 2009, Braun, Huntzinger et al. 2011, Fabian, Cieplak et al. 2011).

Compared to *Cnot6l*, which is ubiquitously expressed in murine organs, *Cnot6* in contrast is expressed specifically and on lower levels in testis, ovary, thymus and spleen (Chen, Ito et al. 2011). In human colon adenocarcinoma *CNOT6L* undergoes a significant copy number loss (Tay, Kats et al. 2011). However, KO mice of both *Cnot6* and *Cnot6l* are viable and fertile (Shirai, Suzuki et al. 2014).

Still, little is known about the function and impact of the CCR4-NOT complex and its components in the heart. Study results vary between showing a significant susceptibility to cardiac hypertrophy and failure of heterozygous *Cnot3* knockout mice in a TAC model and *Cnot3* as an enhancer of human embryonic cardiomyocyte proliferation (Neely, Kuba et al. 2010, Zhou, Liu et al. 2017).
Beside heart specific research, findings in diverse cells reach from observing that knockdown by siRNA of *CNOT6L* leads to a reduced cell survival and proliferation in human MCF7 breast cancer cells by regulating insulin-like growth factor-binding protein 5 and the p53-dependent pathway, to pointing out that the same treatment leads to a significant cell proliferation increase in numerous cell lines (Morita, Suzuki et al. 2007, Mittal, Aslam et al. 2011, Tay, Kats et al. 2011).
To summarize the state of knowledge it seems legitimate to conclude that there is no approved effect of CNOT6L on cell proliferation or growth in scientific literature so far. Since the target recognition of the CCR4-NOT complex works largely by recruitment of numerous microRNAs, the potential target list in different cells, states and reactions is obviously long and yet to considerable extents unknown, although speculations were drawn that it regulates specific sets of genes and conserved pathways like the recruiting microRNAs (Mittal, Aslam et al. 2011).

It has been previously published that *Cnot6l* is targeted by a microRNA. MiR-146a regulates epithelial-mesenchymal transition (EMT) by targeting *Cnot6l* (Zhou and Thiery 2013). As stated before, miR-365 is reported to target Skp2 which regulates protein turnover by autophagy (Wu, Wang et al. 2017). From that, it can be deduced that miR-365 inhibits the decoy of gene products at both the RNA and the protein level. It is of utter importance to note the meaning of this: by binding *Cnot6l* mRNA, microRNA targets its own pathway 'instrument' which is necessary for operation. This should accordingly reduce poly(A)-tail exonuclease-driven mRNA-decay guided by microRNA in general. It is possible that miR-365 regulating *Cnot6l* depicts a restriction of the CCR4-NOT complex miRISC recruitment as a negative feedback loop (Figure 18). Further investigation to quantify the change of total mRNA degradation activity depending on miR-365 manipulation is necessary to clarify this issue.

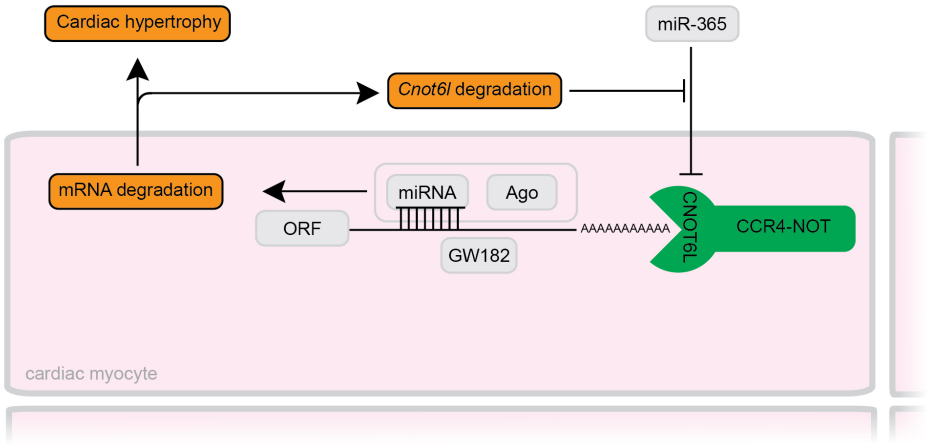

Figure 18: miR-365 CNOT6L negative feedback loop illustration. By targeting *Cnot6l*, miR-365 leads to degradation of the catalytic subunit of the complex it relies on for miRISC (depicted as a complex of miRNA and Ago) activity. MiR-365 supports cardiac hypertrophy by regulation of *Cnot6l.*

4.2 miR-29 and cardiac hypertrophy

4.2.1 Wnt signaling, *Ctnnbip1*, *Glis2* and *Hbp1* in the heart

In this study, it is demonstrated that miR-29 directly targets *Ctnnbip1*, *Glis2* and *Hbp1*. All three genes are signaling members of the Wnt signaling pathway. Wnt pathways

are – as the miR-29 family – evolutionary highly conserved parts in cell signaling. They can be classified in the canonical (or classical, i.e. β-catenin dependent) pathway and in two non-canonical, β-catenin independent pathways. For this study, the canonical pathway is the object of interest (Figure 19).

In its inactivated state, β-catenin is bound in the cytoplasm by Axin which serves as a scaffold protein for a destruction complex, including additionally Glycogen synthase kinase 3 (GSK)-3β, casein kinase (CK)-1α and adenomatous polyposis coli (APC) protein. In this complex, first CK-1α and second GSK-3β phosphorylates β-catenin, facilitating the ubiquitinylation of β-catenin for proteasomal degradation (Amit, Hatzubai et al. 2002). In absence of β-catenin, the transcription factor T-cell factor/lymphoid enhancer factor (TCF/LEF) inhibits the transcription of cell specific Wnt-responsive genes, e.g. the cell cycle regulating genes c-myc and cyclin D. For this inhibition, numerous helper proteins like histone deacetylases (HDAC) and the protein Groucho are necessary.

The canonical pathway is induced by binding of a Wnt ligand, typically WNT1, WNT3A and WNT8 depending on the receptor context, to a Frizzled-receptor (Fzd) (Mikels and Nusse 2006, Kikuchi, Yamamoto et al. 2011). When a Wnt ligand binds the Frizzled-receptor and the low-density lipoprotein receptor-related protein (LRP)5/6, the cytoplasmatic protein Dishevelled-1 (Dvl-1) and Axin are bound to the cell membrane, preventing β-catenin from being phosphorylated (Gao and Chen 2010). β-catenin translocates into the cell nucleus to replace HDAC and Groucho, enabling transcription of the regulated genes (Daniels and Weis 2005).

The β-catenin interacting protein 1 (ICAT, inhibitor of β-catenin and TCF-4, CTNNBIP1), present in the cytoplasm and nucleus, is – independently from the destruction complex – capable of binding β-catenin. The latter is thus unable to displace HDAC and Groucho (Tago, Nakamura et al. 2000, Gottardi and Gumbiner 2004). This leads to its tumor suppressor function as it has been stated by multiple studies. CTNNBIP1 is targeted by several microRNAs (Tong, Liu et al. 2015, Wu, Liu et al. 2015). Recently, it has been shown that miR-29b regulates murine neurogenesis by targeting *Ctnnbip1* and dysregulation leads to defects in corticogenesis (Shin, Shin et al. 2014).

GLIS2, a Kruppel-Like Zinc Finger Protein, seems to have a similar function; by decoying β-catenin primarily in the nucleus, it inhibits Wnt signaling. GLIS2 is highest expressed in the kidney, followed by the heart (Zhang, Nakanishi et al. 2002, Kim, Kang et al. 2007). It participates in different fusion genes in context of acute megakaryoblastic leukemia (Hara, Shiba et al. 2017). The human Glis2 gene is also called NPH7 since its loss of function causes nephronophthisis by increased apoptosis and fibrosis (Attanasio, Uhlenhaut et al. 2007). Progressively, there are reports about the GLIS family regulating cell reprogramming and differentiation for iPSC production (Scoville, Kang et al. 2017).
Even closer to the end of the signal cascade, the HMG-Box transcription factor 1 (HBP1) blocks the transcription of the responsive genes by binding TCF (Sampson, Haque et al. 2001). Recently, it has been observed that HBP1 is targeted by miR-19a in macrophages and promotes atherosclerosis (Chen, Li et al. 2017)
There are no previous reports about CTNNBIP1, GLIS2 or HBP1 in cardiac hypertrophy beside the recent study of our group (Sassi, Avramopoulos et al. 2017).

4.2.2 miR-29 and Wnt signaling in the heart

Since the finding of its first signaling member in 1982, the Wnt pathway is progressively considered as a fundamental regulator of growth, development, differentiation and carcinogenesis. Almost every member of this pathway is described as playing a role in numerous kinds of neoplastic diseases, foremost the APC protein, whose hereditary monoallelic inactivation leads to familial adenomatous polyposis (FAP). In 80% of colorectal cancer the APC gene is mutated, showing the vast impact of this pathway on the cell cycle (Nusse and Varmus 1982, Giles, van Es et al. 2003, Nusse and Clevers 2017).

As a growth and cell division regulating pathway, Wnt signaling is mostly silent in the healthy heart but becomes crucial in multiple pathological reactions, e.g. fibrosis, ventricular remodeling and post-infarction scarring. It has been found that numerous pathway members induce or abrogate these cardiac tissue changes. β-catenin seems to be necessary for cardiac hypertrophy after TAC operation in mice (Chen, Shevtsov et al. 2006, Baurand, Zelarayan et al. 2007, Akhmetshina, Palumbo et al. 2012,

Hermans and Blankesteijn 2015, Tao, Yang et al. 2016, Ma, Zou et al. 2017, Stylianidis, Hermans et al. 2017). Interestingly, the β-catenin conditional knockout display reduced cardiac contractility and function in both TAC and Angiotensin II infusion models. Furthermore, both studies of Chen and Hermans observed a reduction of fibrosis in the concerned animals. This is backed up by another study which observed an upregulation of Wnt signaling in human skin fibroblasts in fibrotic diseases and a reduction of fibrosis in animal models with transgenic overexpression of Dickkopf-1 (Baurand, Zelarayan et al. 2007, Akhmetshina, Palumbo et al. 2012). The described hypertrophic effect of Wnt signaling supports our observation of the hypertrophic effect of miR-29 and its mechanism leading to this effect as well as the concurrently described reduction of fibrosis by Wnt downregulation following the miR-29 knockout *in vivo*. However, our group did not observe a significant increase of cardiac fibrosis (but increased hypertrophy) following miR-29 overexpression *in vivo* (Sassi, Avramopoulos et al. 2017). This could be due to moderately strong performed TAC operations, which resulted in a hypertrophic stimulus but not an end stage heart failure including pronounced fibrosis. In order to unmask other potentially regulated pathways by miR-29 besides Wnt signaling, further investigations are necessary. One way could be an overexpression of miR-29 in an animal model with a conditional knockout of β-catenin.

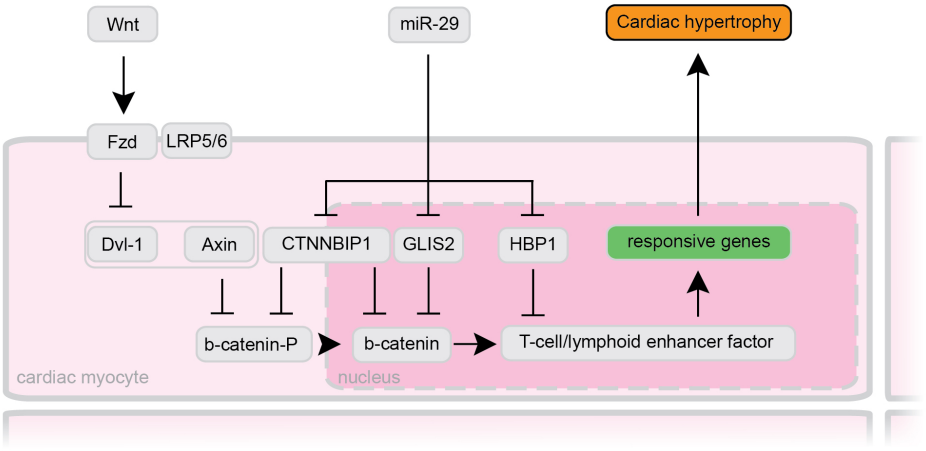

Figure 19: miR-29 directly regulates multiple members of the canonical Wnt-pathway in cardiac myocytes. Illustration of the signal cascade and its pathway members; miR-29 targets CTNNBIP1, GLIS2 and HBP1, which inhibit cardiac hypertrophy via the Wnt pathway

4.2.3 miR-29 and cardiac hypertrophy and fibrosis

The prohypertrophic effect of the miR-29 family was observed before in the screening study (Jentzsch, Leierseder et al. 2012). This effect could be reproduced and confirmed in our group in an *in vivo* setting later on (Sassi, Avramopoulos et al. 2017). Remarkably, this finding is new and contrary to the cardioprotective perspective on the miR-29 family. Up until now, most of the reports were on the regulation of collagen genes in fibroblasts – also in cardiac tissue – by miR-29 (van Rooij, Sutherland et al. 2008, Abonnenc, Nabeebaccus et al. 2013).

Our group assumes that in cardiomyocytes this prohypertrophic effect is primarily due to an upregulation of Wnt signaling by targeting multiple members of this pathway.

In this study, it is shown that three pathway members (*Glis2*, *Hbp1*, *Ctnnbip1*) are directly regulated by the miR-29 family in cardiac myocytes. All three molecules inhibit the interaction of β-catenin with the TCF/LEF-responsive genes in different ways. These results were also confirmed by our group, showing that miR-29 directly regulates these three targets by using a double fluorescent reporter with mutated binding sites as control.

Following these observations, our group implemented *in vivo* that genetic deletion of miR-29 leads to improved cardiac function, reduced cardiac hypertrophy and myocardial fibrosis in a mouse model of cardiac pressure overload.

Furthermore, it is noted that GSK-3β, another key player of the Wnt pathway and NFAT signaling, is targeted by the miR-29 family. MiR-29 overexpression results in a significant reduction in GSK-3β mRNA levels, upregulation of Wnt and NFAT signaling. *In vivo* the mice suffered from increased cardiac hypertrophy and were prone to increased fibrosis.

In the same publication, a massive increase of miR-29 levels in cardiac fibroblasts after cultivation over one week compared to freshly prepared NRCF was documented. With this being an artificial state, culturing the fibroblasts led to an overestimation of the regulatory effect of the miR-29 family compared to effects in other cell types in previous studies. Moreover, our group comes to the conclusion that the Wnt-stimulated cardiomyocytes communicate via paracrine factors with the surrounding cardiac fibroblasts which leads to the profibrotic phenotype – in contrast to the common perspective.

It remains unsettled why one study observed *in vivo* a fibrotic response in cardiac tissue in response to antagomiR-29b after transverse aortic constriction (TAC) operation, even though this phenotype was not objectively quantified (Abonnenc, Nabeebaccus et al. 2013).

If the assumption – also drawn by Abonnenc and van Rooij – of paracrine communication as a main factor for cardiac remodeling (including fibrosis) is correct, it is vital to study the effect of the miR-29 family in a correct cellular context facilitating this paracrine communication. The mentioned proposed bias of miR-29 expression by culturing fibroblasts serves as a good reason for this.

As our study and Abonnenc focused on the pressure overload model by TAC operation, further investigation will be necessary to assess the effect of the miR-29 members on fibrosis and hypertrophy in cardiac tissue in different models (like the ischemia-reperfusion model for myocardial infarction performed by van Rooij, Sutherland et al., 2008).

In summary, this highlights the consequence that one single microRNA can lead to diverse and even oppositional effects depending on the cell type, the cellular and situational context and the microRNA expression level.

In this context, this study laid the basis for a better understanding of the mechanism of action of miR-29 in cardiac tissue.

4.3 Conclusion

Both microRNAs 365 and 29 were found to have a prohypertrophic effect in cardiac myocytes during a phenotypic screening.

This study confirmed the pro-hypertrophic effect of miR-365 *in vitro*, showed the inhibition of the hypertrophic stimuli by the application of antimiR-365 and started a target evaluation. *Cnot6l* as a direct target of miR-365, leading to the observed hypertrophic effect, was identified.

Following the results of the phenotypic screening of our group, several members of the Wnt pathway, i.e. *Ctnnbip1*, *Glis2* and *Hbp1*, were found to be directly targeted by miR-29, contributing to the observed phenotype.

Taken together, these results suggest miR-365 and miR-29 as two important regulators of gene expression in cardiac hypertrophy, which reveals options for future research and new therapeutic starting points.

5 Summary

MicroRNAs are endogenously expressed short RNA molecules (≈22 nucleotides), which modulate gene expression posttranscriptionally by binding mRNA.

Heart failure is a result of continuous excessive stress in cardiac tissue, i.e., mismatch of workload and oxygen supply, triggered by diverse factors. It results in progressive pathologic hypertrophy, marked by unorganized cellular structures as well as increasing fibrosis and declining cardiac function.

Based on an earlier phenotypic screening study, this study shows that two distinct microRNAs exert a strong hypertrophic effect on cardiac myocytes. It is demonstrated that an *in vitro* overexpression of microRNA-365 led to a pro-hypertrophic response in cardiac myocytes. Additionally, a knockdown of miR-365 blocks the response to a hypertrophic stimulus. Moreover, *Cnot6l* as a directly regulated target of miR-365 was identified. Manipulation of both miR-365 and *Cnot6l* regulates hypertrophy. Furthermore, the results point out that the miR-29 family directly regulates several members of the Wnt signaling pathway, which leads to cardiac myocyte hypertrophy. Here the direct regulation of *Glis2*, *Hbp1* and *Ctnnbip1* by miR-29 is shown.

Both microRNAs are strongly hypertrophic molecules in cardiac myocytes. MiR-365 directly targets *Cnot6l*, which contributes to this effect. Targeting these microRNAs could serve as a novel therapeutic strategy in cardiac disease.

6 Zusammenfassung

MicroRNAs sind endogen exprimierte, kurze RNA Moleküle (≈22 Nukleotide), die Genexpression durch posttranskriptionelle Bindung der mRNA regulieren.
Herzinsuffizienz resultiert aus einer längerfristigen und kontinuierlichen Überlastung von Herzgewebe, der ein Missverhältnis von Arbeitsbelastung und Sauerstoffversorgung zugrunde liegt. Dies führt zu progressiver, pathologischer, kardialer Hypertrophie, gekennzeichnet durch unorganisierte Zellverbandstrukturen, Fibrose und eine Abnahme der Herzleistung.
Basierend auf einer früheren Screening-Untersuchung zeigt diese Studie, dass zwei verschiedene MicroRNAs stark hypertrophe Effekte auf das Herzmuskelzellen haben. Es wird gezeigt, dass eine Überexpression von miR-365 *in vitro* eine hypertrophe Reaktion in Herzmuskelzellen zur Folge hat. Ein Knock-down dieser MicroRNA blockierte hingegen hypertrophe Stimuli. Es wurde *Cnot6l* als ein direkt von miR-365 reguliertes Gen identifiziert. Sowohl Manipulation von miR-365 als auch *Cnot6l* regulierte kardiale Hypertrophie *in vitro*. Es wurde außerdem gezeigt, dass die miR-29 Familie zahlreiche Mitglieder des Wnt-Signalwegs direkt reguliert. In dieser Arbeit wird gezeigt, dass *Glis2*, *Hbp1* und *Ctnnbip1* direkt durch miR-29 gesteuert werden.
Es lässt sich aus den Ergebnissen ableiten, dass beide microRNAs einen stark hypertrophen Effekt in Herzmuskelzellen haben. MiR-365 reguliert direkt Cnot6l, was zu diesem Effekt beiträgt.
Diese microRNAs könnten einen neuen Angriffspunkt für die Therapie von Herzinsuffizienz darstellen.

7 Bibliography

Abonnenc, M., A. A. Nabeebaccus, U. Mayr, J. Barallobre-Barreiro, X. Dong, F. Cuello, S. Sur, I. Drozdov, S. R. Langley, R. Lu, K. Stathopoulou, A. Didangelos, X. Yin, W. H. Zimmermann, A. M. Shah, A. Zampetaki and M. Mayr (2013). Extracellular matrix secretion by cardiac fibroblasts: role of microRNA-29b and microRNA-30c. Circ Res 113(10): 1138-1147.

Akhmetshina, A., K. Palumbo, C. Dees, C. Bergmann, P. Venalis, P. Zerr, A. Horn, T. Kireva, C. Beyer, J. Zwerina, H. Schneider, A. Sadowski, M. O. Riener, O. A. MacDougald, O. Distler, G. Schett and J. H. Distler (2012). Activation of canonical Wnt signalling is required for TGF-beta-mediated fibrosis. Nat Commun 3: 735.

Ameres, S. L. and P. D. Zamore (2013). Diversifying microRNA sequence and function. Nat Rev Mol Cell Biol 14(8): 475-488.

Amit, S., A. Hatzubai, Y. Birman, J. S. Andersen, E. Ben-Shushan, M. Mann, Y. Ben-Neriah and I. Alkalay (2002). Axin-mediated CKI phosphorylation of β-catenin at Ser 45: a molecular switch for the Wnt pathway. Genes & Development 16(9): 1066-1076.

Arnold, N., P. R. Koppula, R. Gul, C. Luck and L. Pulakat (2014). Regulation of Cardiac Expression of the Diabetic Marker MicroRNA miR-29. PLoS ONE 9(7): e103284.

Attanasio, M., N. H. Uhlenhaut, V. H. Sousa, J. F. O'Toole, E. Otto, K. Anlag, C. Klugmann, A. C. Treier, J. Helou, J. A. Sayer, D. Seelow, G. Nurnberg, C. Becker, A. E. Chudley, P. Nurnberg, F. Hildebrandt and M. Treier (2007). Loss of GLIS2 causes nephronophthisis in humans and mice by increased apoptosis and fibrosis. Nat Genet 39(8): 1018-1024.

Bartel, D. P. (2009). MicroRNAs: Target Recognition and Regulatory Functions. Cell 136(2): 215-233.

Bashir, T., N. V. Dorrello, V. Amador, D. Guardavaccaro and M. Pagano (2004). Control of the SCF(Skp2-Cks1) ubiquitin ligase by the APC/C(Cdh1) ubiquitin ligase. Nature 428(6979): 190-193.

Baurand, A., L. Zelarayan, R. Betney, C. Gehrke, S. Dunger, C. Noack, A. Busjahn, J. Huelsken, M. M. Taketo, W. Birchmeier, R. Dietz and M. W. Bergmann (2007). Beta-catenin downregulation is required for adaptive cardiac remodeling. Circ Res 100(9): 1353-1362.

Benhamed, M., U. Herbig, T. Ye, A. Dejean and O. Bischof (2012). Senescence is an endogenous trigger for microRNA-directed transcriptional gene silencing in human cells. Nat Cell Biol 14(3): 266-275.

Bhatt, A. B., E. Foster, K. Kuehl, J. Alpert, S. Brabeck, S. Crumb, W. R. Davidson, M. G. Earing, B. B. Ghoshhajra, T. Karamlou, S. Mital, J. Ting and Z. H. Tseng (2015).

Congenital Heart Disease in the Older Adult: A Scientific Statement From the American Heart Association. Circulation.

Bleumink, G. S., A. M. Knetsch, M. C. Sturkenboom, S. M. Straus, A. Hofman, J. W. Deckers, J. C. Witteman and B. H. C. Stricker (2004). Quantifying the heart failure epidemic: prevalence, incidence rate, lifetime risk and prognosis of heart failure The Rotterdam Study. European heart journal 25(18): 1614-1619.

Bonauer, A., G. Carmona, M. Iwasaki, M. Mione, M. Koyanagi, A. Fischer, J. Burchfield, H. Fox, C. Doebele, K. Ohtani, E. Chavakis, M. Potente, M. Tjwa, C. Urbich, A. M. Zeiher and S. Dimmeler (2009). MicroRNA-92a controls angiogenesis and functional recovery of ischemic tissues in mice. Science 324(5935): 1710-1713.

Boon, R. A. and S. Dimmeler (2015). MicroRNAs in myocardial infarction. Nat Rev Cardiol 12(3): 135-142.

Boon, R. A., K. Iekushi, S. Lechner, T. Seeger, A. Fischer, S. Heydt, D. Kaluza, K. Treguer, G. Carmona, A. Bonauer, A. J. G. Horrevoets, N. Didier, Z. Girmatsion, P. Biliczki, J. R. Ehrlich, H. A. Katus, O. J. Muller, M. Potente, A. M. Zeiher, H. Hermeking and S. Dimmeler (2013). MicroRNA-34a regulates cardiac ageing and function. Nature 495(7439): 107-110.

Borchert, G. M., W. Lanier and B. L. Davidson (2006). RNA polymerase III transcribes human microRNAs. Nat Struct Mol Biol 13(12): 1097-1101.

Braun, J. E., E. Huntzinger, M. Fauser and E. Izaurralde (2011). GW182 proteins directly recruit cytoplasmic deadenylase complexes to miRNA targets. Mol Cell 44(1): 120-133.

Brennecke, J., A. Stark, R. B. Russell and S. M. Cohen (2005). Principles of microRNA-target recognition. PLoS Biol 3(3): e85.

Brower, G. L., J. D. Gardner, M. F. Forman, D. B. Murray, T. Voloshenyuk, S. P. Levick and J. S. Janicki (2006). The relationship between myocardial extracellular matrix remodeling and ventricular function. European Journal of Cardio-Thoracic Surgery 30(4): 604-610.

Bundesamt, S. (2014). Todesursachen in Deutschland. Statistisches Bundesamt Fachserie 12 Reihe 4.

Cao, X., J. Wang, Z. Wang, J. Du, X. Yuan, W. Huang, J. Meng, H. Gu, Y. Nie, B. Ji, S. Hu and Z. Zheng (2013). MicroRNA profiling during rat ventricular maturation: A role for miR-29a in regulating cardiomyocyte cell cycle re-entry. FEBS Lett 587(10): 1548-1555.

Carrano, A. C. and M. Pagano (2001). Role of the F-Box Protein Skp2 in Adhesion-Dependent Cell Cycle Progression. J Cell Biol 153(7): 1381-1390.

Chen, C., K. Ito, A. Takahashi, G. Wang, T. Suzuki, T. Nakazawa, T. Yamamoto and K. Yokoyama (2011). Distinct expression patterns of the subunits of the CCR4–NOT

deadenylase complex during neural development. Biochemical and Biophysical Research Communications 411(2): 360-364.

Chen, H., X. Li, S. Liu, L. Gu and X. Zhou (2017). MircroRNA-19a promotes vascular inflammation and foam cell formation by targeting HBP-1 in atherogenesis. Sci Rep 7(1): 12089.

Chen, J. F., E. P. Murchison, R. Tang, T. E. Callis, M. Tatsuguchi, Z. Deng, M. Rojas, S. M. Hammond, M. D. Schneider, C. H. Selzman, G. Meissner, C. Patterson, G. J. Hannon and D. Z. Wang (2008). Targeted deletion of Dicer in the heart leads to dilated cardiomyopathy and heart failure. Proc Natl Acad Sci U S A 105(6): 2111-2116.

Chen, X., S. P. Shevtsov, E. Hsich, L. Cui, S. Haq, M. Aronovitz, R. Kerkela, J. D. Molkentin, R. Liao, R. N. Salomon, R. Patten and T. Force (2006). The beta-catenin/T-cell factor/lymphocyte enhancer factor signaling pathway is required for normal and stress-induced cardiac hypertrophy. Mol Cell Biol 26(12): 4462-4473.

Chen, Z., Z. Huang, Q. Ye, Y. Ming, S. Zhang, Y. Zhao, L. Liu, Q. Wang and K. Cheng (2015). Prognostic significance and anti-proliferation effect of microRNA-365 in hepatocellular carcinoma. Int J Clin Exp Pathol 8(2): 1705-1711.

Chiang, D. Y., N. Kongchan, D. L. Beavers, K. M. Alsina, N. Voigt, J. R. Neilson, H. Jakob, J. F. Martin, D. Dobrev, X. H. T. Wehrens and N. Li (2014). Loss of MicroRNA-106b-25 Cluster Promotes Atrial Fibrillation by Enhancing Ryanodine Receptor Type-2 Expression and Calcium Release. Circulation: Arrhythmia and Electrophysiology 7(6): 1214-1222.

Chiang, D. Y., M. Zhang, N. Voigt, K. M. Alsina, H. Jakob, J. F. Martin, D. Dobrev, X. H. T. Wehrens and N. Li (2015). Identification of microRNA–mRNA dysregulations in paroxysmal atrial fibrillation. International Journal of Cardiology 184(0): 190-197.

Collart, M. A. (2003). Global control of gene expression in yeast by the Ccr4-Not complex. Gene 313(0): 1-16.

Cushing, L., P. Kuang and J. Lü (2014). The role of miR-29 in pulmonary fibrosis. Biochemistry and Cell Biology 93(2): 109-118.

Daimi, H., E. Lozano-Velasco, A. Haj Khelil, J. B. Chibani, A. Barana, I. Amoros, M. Gonzalez de la Fuente, R. Caballero, A. Aranega and D. Franco (2015). Regulation of SCN5A by microRNAs: miR-219 modulates SCN5A transcript expression and the effects of flecainide intoxication in mice. Heart Rhythm.

Daniels, D. L. and W. I. Weis (2005). [beta]-catenin directly displaces Groucho/TLE repressors from Tcf/Lef in Wnt-mediated transcription activation. Nat Struct Mol Biol 12(4): 364-371.

Ding, D.-P., Z.-L. Chen, X.-H. Zhao, J.-W. Wang, J. Sun, Z. Wang, F.-W. Tan, X.-G. Tan, B.-Z. Li, F. Zhou, K. Shao, N. Li, B. Qiu and J. He (2011). miR-29c induces cell cycle arrest in esophageal squamous cell carcinoma by modulating cyclin E expression. Carcinogenesis 32(7): 1025-1032.

Dirkx, E., P. A. da Costa Martins and L. J. De Windt (2013). Regulation of fetal gene expression in heart failure. Biochimica et Biophysica Acta (BBA) - Molecular Basis of Disease 1832(12): 2414-2424.

Dmitriev, P., L. Stankevicins, E. Ansseau, A. Petrov, A. Barat, P. Dessen, T. Robert, A. Turki, V. Lazar, E. Labourer, A. Belayew, G. Carnac, D. Laoudj-Chenivesse, M. Lipinski and Y. S. Vassetzky (2013). Defective regulation of microRNA target genes in myoblasts from facioscapulohumeral dystrophy patients. J Biol Chem 288(49): 34989-35002.

Duong, E., J. Xiao, X. Y. Qi and S. Nattel (2017). MicroRNA-135a regulates sodium-calcium exchanger gene expression and cardiac electrical activity. Heart Rhythm 14(5): 739-748.

Fabbri, M., R. Garzon, A. Cimmino, Z. Liu, N. Zanesi, E. Callegari, S. Liu, H. Alder, S. Costinean, C. Fernandez-Cymering, S. Volinia, G. Guler, C. D. Morrison, K. K. Chan, G. Marcucci, G. A. Calin, K. Huebner and C. M. Croce (2007). MicroRNA-29 family reverts aberrant methylation in lung cancer by targeting DNA methyltransferases 3A and 3B. Proceedings of the National Academy of Sciences 104(40): 15805-15810.

Fabian, M. R., M. K. Cieplak, F. Frank, M. Morita, J. Green, T. Srikumar, B. Nagar, T. Yamamoto, B. Raught, T. F. Duchaine and N. Sonenberg (2011). miRNA-mediated deadenylation is orchestrated by GW182 through two conserved motifs that interact with CCR4–NOT. Nat Struct Mol Biol 18(11): 1211-1217.

Fabian, M. R., G. Mathonnet, T. Sundermeier, H. Mathys, J. T. Zipprich, Y. V. Svitkin, F. Rivas, M. Jinek, J. Wohlschlegel, J. A. Doudna, C.-Y. A. Chen, A.-B. Shyu, J. R. Yates Iii, G. J. Hannon, W. Filipowicz, T. F. Duchaine and N. Sonenberg (2009). Mammalian miRNA RISC Recruits CAF1 and PABP to Affect PABP-Dependent Deadenylation. Molecular Cell 35(6): 868-880.

Feuermann, Y., K. Kang, O. Gavrilova, N. Haetscher, S. J. Jang, K. H. Yoo, C. Jiang, F. J. Gonzalez, G. W. Robinson and L. Hennighausen (2013). MiR-193b and miR-365-1 are not required for the development and function of brown fat in the mouse. RNA Biol 10(12): 1807-1814.

Frohlich, E. D., C. Apstein, A. V. Chobanian, R. B. Devereux, H. P. Dustan, V. Dzau, F. Fauad-Tarazi, M. J. Horan, M. Marcus, B. Massie, M. A. Pfeffer, R. N. Re, E. J. Roccella, D. Savage and C. Shub (1992). The Heart in Hypertension. New England Journal of Medicine 327(14): 998-1008.

Ganesan, J., D. Ramanujam, Y. Sassi, A. Ahles, C. Jentzsch, S. Werfel, S. Leierseder, X. Loyer, M. Giacca, L. Zentilin, T. Thum, B. Laggerbauer and S. Engelhardt (2013). MiR-378 Controls Cardiac Hypertrophy by Combined Repression of Mitogen-Activated Protein Kinase Pathway Factors. Circulation 127(21): 2097-2106.

Gao, C. and Y.-G. Chen (2010). Dishevelled: The hub of Wnt signaling. Cellular Signalling 22(5): 717-727.

Gebeshuber, C. A., K. Zatloukal and J. Martinez (2009). miR-29a suppresses tristetraprolin, which is a regulator of epithelial polarity and metastasis. EMBO reports 10(4): 400-405.

Giles, R. H., J. H. van Es and H. Clevers (2003). Caught up in a Wnt storm: Wnt signaling in cancer. Biochimica et Biophysica Acta (BBA) - Reviews on Cancer 1653(1): 1-24.

Gopal, M. and B. Karnath (2009). Clinical diagnosis of heart failure. Hospital Physician 45(7): 9-15.

Gottardi, C. J. and B. M. Gumbiner (2004). Role for ICAT in β-catenin-dependent nuclear signaling and cadherin functions. American Journal of Physiology - Cell Physiology 286(4): C747-C756.

Gregory, R. I., K.-p. Yan, G. Amuthan, T. Chendrimada, B. Doratotaj, N. Cooch and R. Shiekhattar (2004). The Microprocessor complex mediates the genesis of microRNAs. Nature 432(7014): 235-240.

Grossman, W., D. Jones and L. P. McLaurin (1975). Wall stress and patterns of hypertrophy in the human left ventricle. The Journal of Clinical Investigation 56(1): 56-64.

Guan, Y.-J., X. Yang, L. Wei and Q. Chen (2011). MiR-365: a mechanosensitive microRNA stimulates chondrocyte differentiation through targeting histone deacetylase 4. The FASEB Journal 25(12): 4457-4466.

Guo, S.-L., H. Ye, Y. Teng, Y.-L. Wang, G. Yang, X.-B. Li, C. Zhang, X. Yang, Z.-Z. Yang and X. Yang (2013). Akt-p53-miR-365-cyclin D1/cdc25A axis contributes to gastric tumorigenesis induced by PTEN deficiency. Nat Commun 4.

Hamada, S., A. Masamune, S. Miura, K. Satoh and T. Shimosegawa (2014). MiR-365 induces gemcitabine resistance in pancreatic cancer cells by targeting the adaptor protein SHC1 and pro-apoptotic regulator BAX. Cellular Signalling 26(2): 179-185.

Hara, Y., N. Shiba, K. Ohki, K. Tabuchi, G. Yamato, M. J. Park, D. Tomizawa, A. Kinoshita, A. Shimada, H. Arakawa, A. M. Saito, N. Kiyokawa, A. Tawa, K. Horibe, T. Taga, S. Adachi, T. Taki and Y. Hayashi (2017). Prognostic impact of specific molecular profiles in pediatric acute megakaryoblastic leukemia in non-Down syndrome. Genes Chromosomes Cancer 56(5): 394-404.

Hergenreider, E., S. Heydt, K. Treguer, T. Boettger, A. J. G. Horrevoets, A. M. Zeiher, M. P. Scheffer, A. S. Frangakis, X. Yin, M. Mayr, T. Braun, C. Urbich, R. A. Boon and S. Dimmeler (2012). Atheroprotective communication between endothelial cells and smooth muscle cells through miRNAs. Nat Cell Biol 14(3): 249-256.

Hermans, K. C. and W. M. Blankesteijn (2015). Wnt Signaling in Cardiac Disease. Compr Physiol 5(3): 1183-1209.

Hill, J. A. and E. N. Olson (2008). Cardiac Plasticity. New England Journal of Medicine 358(13): 1370-1380.

Hong, B., H. Li, M. Zhang, J. Xu, Y. Lu, Y. Zheng, J. Qian, J. T. Chang, J. Yang and Q. Yi (2015). p38 MAPK inhibits breast cancer metastasis through regulation of stromal expansion. International Journal of Cancer 136(1): 34-43.

Hullinger, T. G., R. L. Montgomery, A. G. Seto, B. A. Dickinson, H. M. Semus, J. M. Lynch, C. M. Dalby, K. Robinson, C. Stack, P. A. Latimer, J. M. Hare, E. N. Olson and E. van Rooij (2012). Inhibition of miR-15 Protects Against Cardiac Ischemic Injury. Circulation Research 110(1): 71-81.

Hunter, J. J. and K. R. Chien (1999). Signaling Pathways for Cardiac Hypertrophy and Failure. New England Journal of Medicine 341(17): 1276-1283.

Huntzinger, E. and E. Izaurralde (2011). Gene silencing by microRNAs: contributions of translational repression and mRNA decay. Nat Rev Genet 12(2): 99-110.

Hutvagner, G. and P. D. Zamore (2002). A microRNA in a multiple-turnover RNAi enzyme complex. Science 297(5589): 2056-2060.

Hwang, H.-W., E. A. Wentzel and J. T. Mendell (2007). A Hexanucleotide Element Directs MicroRNA Nuclear Import. Science 315(5808): 97-100.

Iaconetti, C., A. Polimeni, S. Sorrentino, J. Sabatino, G. Pironti, G. Esposito, A. Curcio and C. Indolfi (2012). Inhibition of miR-92a increases endothelial proliferation and migration in vitro as well as reduces neointimal proliferation in vivo after vascular injury. Basic Research in Cardiology 107(5): 1-14.

Jentzsch, C., S. Leierseder, X. Loyer, I. Flohrschütz, Y. Sassi, D. Hartmann, T. Thum, B. Laggerbauer and S. Engelhardt (2012). A phenotypic screen to identify hypertrophy-modulating microRNAs in primary cardiomyocytes. Journal of Molecular and Cellular Cardiology 52(1): 13-20.

Kang, S.-M., H.-J. Lee and J.-Y. Cho (2013). MicroRNA-365 regulates NKX2-1, a key mediator of lung cancer. Cancer Letters 335(2): 487-494.

Kannel, W. B. and A. J. Belanger (1991). Epidemiology of heart failure. American Heart Journal 121(3, Part 1): 951-957.

Kawamata, T. and Y. Tomari (2010). Making RISC. Trends in Biochemical Sciences 35(7): 368-376.

Kenchaiah, S., J. Narula and R. S. Vasan (2004). Risk factors for heart failure. Med Clin North Am 88(5): 1145-1172.

Kikuchi, A., H. Yamamoto, A. Sato and S. Matsumoto (2011). Chapter 2 - New Insights into the Mechanism of Wnt Signaling Pathway Activation. International Review of Cell and Molecular Biology. W. J. Kwang, Academic Press. Volume 291: 21-71.

Kim, G. H. (2013). MicroRNA regulation of cardiac conduction and arrhythmias. Transl Res 161(5): 381-392.

Kim, Y.-S., H. S. Kang and A. M. Jetten (2007). The Krüppel-like zinc finger protein Glis2 functions as a negative modulator of the Wnt/β-catenin signaling pathway. FEBS Letters 581(5): 858-864.

Krayenbuehl, H., O. Hess, J. Schneider and M. Turina (1983). Physiologic or pathologic hypertrophy. European heart journal 4(suppl A): 29-34.

Kuersten, S. and E. B. Goodwin (2003). The power of the 3' UTR: translational control and development. Nat Rev Genet 4(8): 626-637.

Lagos-Quintana, M., R. Rauhut, W. Lendeckel and T. Tuschl (2001). Identification of novel genes coding for small expressed RNAs. Science 294(5543): 853-858.

Lau, N. C., L. P. Lim, E. G. Weinstein and D. P. Bartel (2001). An abundant class of tiny RNAs with probable regulatory roles in Caenorhabditis elegans. Science 294(5543): 858-862.

Lee, R. C. and V. Ambros (2001). An extensive class of small RNAs in Caenorhabditis elegans. Science 294(5543): 862-864.

Lee, R. C., R. L. Feinbaum and V. Ambros (1993). The C. elegans heterochronic gene lin-4 encodes small RNAs with antisense complementarity to lin-14. Cell 75(5): 843-854.

Lee, Y., C. Ahn, J. Han, H. Choi, J. Kim, J. Yim, J. Lee, P. Provost, O. Radmark, S. Kim and V. N. Kim (2003). The nuclear RNase III Drosha initiates microRNA processing. Nature 425(6956): 415-419.

Lee, Y., M. Kim, J. Han, K. H. Yeom, S. Lee, S. H. Baek and V. N. Kim (2004). MicroRNA genes are transcribed by RNA polymerase II. EMBO J 23(20): 4051-4060.

Lin, B., D. G. Feng, F. Wang, J. X. Wang, C. G. Xu, H. Zhao and Z. Y. Cheng (2016). MiR-365 participates in coronary atherosclerosis through regulating IL-6. Eur Rev Med Pharmacol Sci 20(24): 5186-5192.

Little, B. (1994). The Criteria Committee of the New York Heart Association. Nomenclature and criteria for diagnosis and diseases of the heart and great vessels. 9th edition. Boston.

Lund, E., S. Guttinger, A. Calado, J. E. Dahlberg and U. Kutay (2004). Nuclear export of microRNA precursors. Science 303(5654): 95-98.

Ma, Y., H. Zou, X. X. Zhu, J. Pang, Q. Xu, Q. Y. Jin, Y. H. Ding, B. Zhou and D. S. Huang (2017). Transforming growth factor beta: A potential biomarker and therapeutic target of ventricular remodeling. Oncotarget.

Mahmood, S. S. and T. J. Wang (2013). The epidemiology of congestive heart failure: the Framingham Heart Study perspective. Glob Heart 8(1): 77-82.

Mathers, C. D. and D. Loncar (2006). Projections of global mortality and burden of disease from 2002 to 2030. PLoS Med 3(11): e442.

McKee, P. A., W. P. Castelli, P. M. McNamara and W. B. Kannel (1971). The Natural History of Congestive Heart Failure: The Framingham Study. New England Journal of Medicine 285(26): 1441-1446.

McMullen, J. R. and G. L. Jennings (2007). Differences between pathological and physiological cardiac hypertrophy: novel therapeutic strategies to treat heart failure. Clin Exp Pharmacol Physiol 34(4): 255-262.

Meister, G., M. Landthaler, L. Peters, P. Y. Chen, H. Urlaub, R. Lührmann and T. Tuschl (2005). Identification of Novel Argonaute-Associated Proteins. Current Biology 15(23): 2149-2155.

Meng, X.-M., P. M.-K. Tang, J. Li and H. Y. Lan (2015). TGF-β/Smad signaling in renal fibrosis. Frontiers in Physiology 6.

Meunier, J., F. Lemoine, M. Soumillon, A. Liechti, M. Weier, K. Guschanski, H. Hu, P. Khaitovich and H. Kaessmann (2013). Birth and expression evolution of mammalian microRNA genes. Genome Res 23(1): 34-45.

Mikels, A. J. and R. Nusse (2006). Purified Wnt5a Protein Activates or Inhibits β-Catenin–TCF Signaling Depending on Receptor Context. PLoS Biol 4(4): e115.

Mittal, S., A. Aslam, R. Doidge, R. Medica and G. S. Winkler (2011). The Ccr4a (CNOT6) and Ccr4b (CNOT6L) deadenylase subunits of the human Ccr4-Not complex contribute to the prevention of cell death and senescence. Mol Biol Cell 22(6): 748-758.

Montgomery, R. L., G. Yu, P. A. Latimer, C. Stack, K. Robinson, C. M. Dalby, N. Kaminski and E. van Rooij (2014). MicroRNA mimicry blocks pulmonary fibrosis. EMBO Molecular Medicine 6(10): 1347-1356.

Mori, M. A., T. Thomou, J. Boucher, K. Y. Lee, S. Lallukka, J. K. Kim, M. Torriani, J. Yki, xE, H. rvinen, S. K. Grinspoon, A. M. Cypess and C. R. Kahn (2014). Altered miRNA processing disrupts brown/white adipocyte determination and associates with lipodystrophy. The Journal of Clinical Investigation 124(8): 3339-3351.

Morita, M., T. Suzuki, T. Nakamura, K. Yokoyama, T. Miyasaka and T. Yamamoto (2007). Depletion of mammalian CCR4b deadenylase triggers elevation of the p27Kip1 mRNA level and impairs cell growth. Mol Cell Biol 27(13): 4980-4990.

Mott, J. L., S. Kobayashi, S. F. Bronk and G. J. Gores (2007). mir-29 regulates Mcl-1 protein expression and apoptosis. Oncogene 26(42): 6133-6140.

Mueller, C., B. Frana, D. Rodriguez, K. Laule-Kilian and A. P. Perruchoud (2005). Emergency diagnosis of congestive heart failure: impact of signs and symptoms. The Canadian journal of cardiology 21(11): 921-924.

Neely, G. G., K. Kuba, A. Cammarato, K. Isobe, S. Amann, L. Zhang, M. Murata, L. Elmen, V. Gupta, S. Arora, R. Sarangi, D. Dan, S. Fujisawa, T. Usami, C. P. Xia, A. C. Keene, N. N. Alayari, H. Yamakawa, U. Elling, C. Berger, M. Novatchkova, R. Koglgruber, K. Fukuda, H. Nishina, M. Isobe, J. A. Pospisilik, Y. Imai, A. Pfeufer, A. A.

Hicks, P. P. Pramstaller, S. Subramaniam, A. Kimura, K. Ocorr, R. Bodmer and J. M. Penninger (2010). A global in vivo Drosophila RNAi screen identifies NOT3 as a conserved regulator of heart function. Cell 141(1): 142-153.

Nicolini, G., F. Forini, C. Kusmic, L. Pitto, L. Mariani and G. Iervasi (2015). Early and short-term triiodothyronine supplementation prevents adverse post-ischemic cardiac remodeling: role of transforming growth factor-beta1 and anti-fibrotic miRNA signaling. Mol Med.

Nie, J., L. Liu, W. Zheng, L. Chen, X. Wu, Y. Xu, X. Du and W. Han (2012). microRNA-365, down-regulated in colon cancer, inhibits cell cycle progression and promotes apoptosis of colon cancer cells by probably targeting Cyclin D1 and Bcl-2. Carcinogenesis 33(1): 220-225.

Nusse, R. and H. Clevers (2017). Wnt/beta-Catenin Signaling, Disease, and Emerging Therapeutic Modalities. Cell 169(6): 985-999.

Nusse, R. and H. E. Varmus (1982). Many tumors induced by the mouse mammary tumor virus contain a provirus integrated in the same region of the host genome. Cell 31(1): 99-109.

Okamura, K., M. D. Phillips, D. M. Tyler, H. Duan, Y. T. Chou and E. C. Lai (2008). The regulatory activity of microRNA* species has substantial influence on microRNA and 3' UTR evolution. Nat Struct Mol Biol 15(4): 354-363.

Olson, E. N. (2006). Gene regulatory networks in the evolution and development of the heart. Science 313(5795): 1922-1927.

Organization, W. H. (2014). Global status report on noncommunicable diseases 2014. World Health Organization.

Osbourne, A., T. Calway, M. Broman, S. McSharry, J. Earley and G. H. Kim (2014). Downregulation of connexin43 by microRNA-130a in cardiomyocytes results in cardiac arrhythmias. Journal of Molecular and Cellular Cardiology 74(0): 53-63.

Park, S.-Y., J. H. Lee, M. Ha, J.-W. Nam and V. N. Kim (2009). miR-29 miRNAs activate p53 by targeting p85[alpha] and CDC42. Nat Struct Mol Biol 16(1): 23-29.

Pasquinelli, A. E. (2012). MicroRNAs and their targets: recognition, regulation and an emerging reciprocal relationship. Nat Rev Genet 13(4): 271-282.

Pluim, B. M., A. H. Zwinderman, A. van der Laarse and E. E. van der Wall (2000). The Athlete's Heart: A Meta-Analysis of Cardiac Structure and Function. Circulation 101(3): 336-344.

Qi, J., S. J. Rice, A. C. Salzberg, E. A. Runkle, J. Liao, D. S. Zander and D. Mu (2012). MiR-365 regulates lung cancer and developmental gene thyroid transcription factor 1. Cell Cycle 11(1): 177-186.

Ramdas, V., M. McBride, L. Denby and A. H. Baker (2013). Canonical Transforming Growth Factor-β Signaling Regulates Disintegrin Metalloprotease Expression in

Experimental Renal Fibrosis via miR-29. The American Journal of Pathology 183(6): 1885-1896.

Robb, G. B. and T. M. Rana (2007). RNA Helicase A Interacts with RISC in Human Cells and Functions in RISC Loading. Molecular Cell 26(4): 523-537.

Rothschild, S. I., M. P. Tschan, E. A. Federzoni, R. Jaggi, M. F. Fey, M. Gugger and O. Gautschi (2012). MicroRNA-29b is involved in the Src-ID1 signaling pathway and is dysregulated in human lung adenocarcinoma. Oncogene 31(38): 4221-4232.

Sampson, E. M., Z. K. Haque, M. C. Ku, S. G. Tevosian, C. Albanese, R. G. Pestell, K. E. Paulson and A. S. Yee (2001). Negative regulation of the Wnt–β-catenin pathway by the transcriptional repressor HBP1. The EMBO Journal 20(16): 4500-4511.

Sassi, Y., P. Avramopoulos, D. Ramanujam, L. Gruter, S. Werfel, S. Giosele, A. D. Brunner, D. Esfandyari, A. S. Papadopoulou, B. De Strooper, N. Hubner, R. Kumarswamy, T. Thum, X. Yin, M. Mayr, B. Laggerbauer and S. Engelhardt (2017). Cardiac myocyte miR-29 promotes pathological remodeling of the heart by activating Wnt signaling. Nat Commun 8(1): 1614.

Saxena, A. and C. J. Tabin (2010). miRNA-processing enzyme Dicer is necessary for cardiac outflow tract alignment and chamber septation. Proc Natl Acad Sci U S A 107(1): 87-91.

Schocken, D. D., E. J. Benjamin, G. C. Fonarow, H. M. Krumholz, D. Levy, G. A. Mensah, J. Narula, E. S. Shor, J. B. Young and Y. Hong (2008). Prevention of heart failure: a scientific statement from the American Heart Association Councils on Epidemiology and Prevention, Clinical Cardiology, Cardiovascular Nursing, and High Blood Pressure Research; Quality of Care and Outcomes Research Interdisciplinary Working Group; and Functional Genomics and Translational Biology Interdisciplinary Working Group. Circulation 117(19): 2544-2565.

Scoville, D. W., H. S. Kang and A. M. Jetten (2017). GLIS1-3: emerging roles in reprogramming, stem and progenitor cell differentiation and maintenance. Stem Cell Investig 4: 80.

Seviour, E. G., V. Sehgal, Y. Lu, Z. Luo, T. Moss, F. Zhang, S. M. Hill, W. Liu, S. N. Maiti, L. Cooper, R. Azencot, G. Lopez-Berestein, C. Rodriguez-Aguayo, R. Roopaimoole, C. Pecot, A. K. Sood, S. Mukherjee, J. W. Gray, G. B. Mills and P. T. Ram (2015). Functional proteomics identifies miRNAs to target a p27/Myc/phospho-Rb signature in breast and ovarian cancer. Oncogene.

Shin, J., Y. Shin, S. M. Oh, H. Yang, W. J. Yu, J. P. Lee, S. O. Huh, S. H. Lee, Y. H. Suh, S. Chung and H. S. Kim (2014). MiR-29b controls fetal mouse neurogenesis by regulating ICAT-mediated Wnt/[beta]-catenin signaling. Cell Death Dis 5: e1473.

Shirai, Y.-T., T. Suzuki, M. Morita, A. Takahashi and T. Yamamoto (2014). Multifunctional roles of the mammalian CCR4-NOT complex in physiological phenomena. Frontiers in Genetics 5.

Small, E. M., R. J. Frost and E. N. Olson (2010). MicroRNAs add a new dimension to cardiovascular disease. Circulation 121(8): 1022-1032.

Stevenson, L. and J. K. Perloff (1989). THe limited reliability of physical signs for estimating hemodynamics in chronic heart failure. JAMA 261(6): 884-888.

Stylianidis, V., K. C. M. Hermans and W. M. Blankesteijn (2017). Wnt Signaling in Cardiac Remodeling and Heart Failure. Handb Exp Pharmacol 243: 371-393.

Tago, K.-i., T. Nakamura, M. Nishita, J. Hyodo, S.-i. Nagai, Y. Murata, S. Adachi, S. Ohwada, Y. Morishita, H. Shibuya and T. Akiyama (2000). Inhibition of Wnt signaling by ICAT, a novel β-catenin-interacting protein. Genes & Development 14(14): 1741-1749.

Tan, J., B.-D. Tong, Y.-J. Wu and W. Xiong (2014). MicroRNA-29 mediates TGFβ1-induced extracellular matrix synthesis by targeting wnt/β-catenin pathway in human orbital fibroblasts. International Journal of Clinical and Experimental Pathology 7(11): 7571-7577.

Tao, H., J. J. Yang, K. H. Shi and J. Li (2016). Wnt signaling pathway in cardiac fibrosis: New insights and directions. Metabolism 65(2): 30-40.

Tay, Y., L. Kats, L. Salmena, D. Weiss, Shen M. Tan, U. Ala, F. Karreth, L. Poliseno, P. Provero, F. Di Cunto, J. Lieberman, I. Rigoutsos and Pier P. Pandolfi (2011). Coding-Independent Regulation of the Tumor Suppressor PTEN by Competing Endogenous mRNAs. Cell 147(2): 344-357.

Thum, T., C. Gross, J. Fiedler, T. Fischer, S. Kissler, M. Bussen, P. Galuppo, S. Just, W. Rottbauer, S. Frantz, M. Castoldi, J. Soutschek, V. Koteliansky, A. Rosenwald, M. A. Basson, J. D. Licht, J. T. R. Pena, S. H. Rouhanifard, M. U. Muckenthaler, T. Tuschl, G. R. Martin, J. Bauersachs and S. Engelhardt (2008). MicroRNA-21 contributes to myocardial disease by stimulating MAP kinase signalling in fibroblasts. Nature 456(7224): 980-984.

Tolia, N. H. and L. Joshua-Tor (2007). Slicer and the Argonautes. Nat Chem Biol 3(1): 36-43.

Tong, Y. Q., B. Liu, H. Y. Zheng, J. Gu, H. Liu, F. Li, B. H. Tan, M. Hartman, C. Song and Y. Li (2015). MiR-215, an activator of the CTNNBIP1/beta-catenin pathway, is a marker of poor prognosis in human glioma. Oncotarget 6(28): 25024-25033.

van Rooij, E., D. Quiat, B. A. Johnson, L. B. Sutherland, X. Qi, J. A. Richardson, R. J. Kelm, Jr. and E. N. Olson (2009). A family of microRNAs encoded by myosin genes governs myosin expression and muscle performance. Dev Cell 17(5): 662-673.

van Rooij, E., L. B. Sutherland, X. Qi, J. A. Richardson, J. Hill and E. N. Olson (2007). Control of stress-dependent cardiac growth and gene expression by a microRNA. Science 316(5824): 575-579.

van Rooij, E., L. B. Sutherland, J. E. Thatcher, J. M. DiMaio, R. H. Naseem, W. S. Marshall, J. A. Hill and E. N. Olson (2008). Dysregulation of microRNAs after

myocardial infarction reveals a role of miR-29 in cardiac fibrosis. Proc Natl Acad Sci U S A 105(35): 13027-13032.

Viereck, J., C. Bang, A. Foinquinos and T. Thum (2014). Regulatory RNAs and paracrine networks in the heart. Cardiovasc Res 102(2): 290-301.

Wang, C., C. Gao, J.-L. Zhuang, C. Ding and Y. Wang (2012). A combined approach identifies three mRNAs that are down-regulated by microRNA-29b and promote invasion ability in the breast cancer cell line MCF-7. Journal of Cancer Research and Clinical Oncology 138(12): 2127-2136.

Wang, H., M. Morita, X. Yang, T. Suzuki, W. Yang, J. Wang, K. Ito, Q. Wang, C. Zhao, M. Bartlam, T. Yamamoto and Z. Rao (2010). Crystal structure of the human CNOT6L nuclease domain reveals strict poly(A) substrate specificity. The EMBO Journal 29(15): 2566-2576.

Weber, K. T., W. A. Clark, J. S. Janicki and S. G. Shroff (1987). Physiologic Versus Pathologic Hypertrophy and the Pressure-Overloaded Myocardium. Journal of Cardiovascular Pharmacology 10: S37-S50.

Widera, C., S. K. Gupta, J. M. Lorenzen, C. Bang, J. Bauersachs, K. Bethmann, T. Kempf, K. C. Wollert and T. Thum (2011). Diagnostic and prognostic impact of six circulating microRNAs in acute coronary syndrome. J Mol Cell Cardiol 51(5): 872-875.

Winter, J., S. Jung, S. Keller, R. I. Gregory and S. Diederichs (2009). Many roads to maturity: microRNA biogenesis pathways and their regulation. Nat Cell Biol 11(3): 228-234.

Wu, G., A. Liu, J. Zhu, F. Lei, S. Wu, X. Zhang, L. Ye, L. Cao and S. He (2015). MiR-1207 overexpression promotes cancer stem cell-like traits in ovarian cancer by activating the Wnt/beta-catenin signaling pathway. Oncotarget 6(30): 28882-28894.

Wu, H., Y. Wang, X. Wang, R. Li and D. Yin (2017). MicroRNA-365 accelerates cardiac hypertrophy by inhibiting autophagy via the modulation of Skp2 expression. Biochemical and Biophysical Research Communications 484(2): 304-310.

Xiong, X.-d., H. J. Jung, S. Gombar, J. Y. Park, C.-l. Zhang, H. Zheng, J. Ruan, J.-b. Li, M. Kaeberlein, B. K. Kennedy, Z. Zhou, X. Liu and Y. Suh (2015). MicroRNA transcriptome analysis identifies miR-365 as a novel negative regulator of cell proliferation in Zmpste24-deficient mouse embryonic fibroblasts. Mutation Research/Fundamental and Molecular Mechanisms of Mutagenesis 777(0): 69-78.

Xu, Z., S.-B. Xiao, P. Xu, Q. Xie, L. Cao, D. Wang, R. Luo, Y. Zhong, H.-C. Chen and L.-R. Fang (2011). miR-365, a Novel Negative Regulator of Interleukin-6 Gene Expression, Is Cooperatively Regulated by Sp1 and NF-κB. Journal of Biological Chemistry 286(24): 21401-21412.

Yamashita, A., T.-C. Chang, Y. Yamashita, W. Zhu, Z. Zhong, C.-Y. A. Chen and A.-B. Shyu (2005). Concerted action of poly(A) nucleases and decapping enzyme in mammalian mRNA turnover. Nat Struct Mol Biol 12(12): 1054-1063.

Yancy, C. W., M. Jessup, B. Bozkurt, J. Butler, D. E. Casey, M. H. Drazner, G. C. Fonarow, S. A. Geraci, T. Horwich and J. L. Januzzi (2013). 2013 ACCF/AHA guideline for the management of heart failure: a report of the American College of Cardiology Foundation/American Heart Association Task Force on Practice Guidelines. Journal of the American College of Cardiology 62(16): e147-e239.

Yang, B., H. Lin, J. Xiao, Y. Lu, X. Luo, B. Li, Y. Zhang, C. Xu, Y. Bai, H. Wang, G. Chen and Z. Wang (2007). The muscle-specific microRNA miR-1 regulates cardiac arrhythmogenic potential by targeting GJA1 and KCNJ2. Nat Med 13(4): 486-491.

Yang, J. S. and E. C. Lai (2011). Alternative miRNA biogenesis pathways and the interpretation of core miRNA pathway mutants. Mol Cell 43(6): 892-903.

Yekta, S., I. H. Shih and D. P. Bartel (2004). MicroRNA-directed cleavage of HOXB8 mRNA. Science 304(5670): 594-596.

Yi, R., Y. Qin, I. G. Macara and B. R. Cullen (2003). Exportin-5 mediates the nuclear export of pre-microRNAs and short hairpin RNAs. Genes Dev 17(24): 3011-3016.

Yu, B. and H. Wang (2010). Translational inhibition by microRNAs in plants. Prog Mol Subcell Biol 50: 41-57.

Zanotti, S., S. Gibertini, M. Curcio, P. Savadori, B. Pasanisi, L. Morandi, F. Cornelio, R. Mantegazza and M. Mora (2015). Opposing roles of miR-21 and miR-29 in the progression of fibrosis in Duchenne muscular dystrophy. Biochimica et Biophysica Acta (BBA) - Molecular Basis of Disease 1852(7): 1451-1464.

Zeng, Y. and B. R. Cullen (2003). Sequence requirements for micro RNA processing and function in human cells. RNA 9(1): 112-123.

Zhang, F., G. Nakanishi, S. Kurebayashi, K. Yoshino, A. Perantoni, Y.-S. Kim and A. M. Jetten (2002). Characterization of Glis2, a Novel Gene Encoding a Gli-related, Krüppel-like Transcription Factor with Transactivation and Repressor Functions: ROLES IN KIDNEY DEVELOPMENT AND NEUROGENESIS. Journal of Biological Chemistry 277(12): 10139-10149.

Zhang, Y., X.-R. Huang, L.-H. Wei, A. C. K. Chung, C.-M. Yu and H.-Y. Lan (2014). miR-29b as a Therapeutic Agent for Angiotensin II-induced Cardiac Fibrosis by Targeting TGF-[beta]/Smad3 signaling. Mol Ther 22(5): 974-985.

Zhou, B., J. Liu, Z. Ren, F. Yao, J. Ma, J. Song, B. Bennett, Y. Zhen, L. Wang, G. Hu and S. Hu (2017). Cnot3 enhances human embryonic cardiomyocyte proliferation by promoting cell cycle inhibitor mRNA degradation. Sci Rep 7(1): 1500.

Zhou, M., W. Liu, S. Ma, H. Cao, X. Peng, L. Guo, X. Zhou, L. Zheng, L. Guo, M. Wan, W. Shi, Y. He, C. Lu, L. Jiang, C. Ou, Y. Guo and Z. Ding (2013). A novel onco-miR-365 induces cutaneous squamous cell carcinoma. Carcinogenesis 34(7): 1653-1659.

Zhou, M., L. Zhou, L. Zheng, L. Guo, Y. Wang, H. Liu, C. Ou and Z. Ding (2014). miR-365 Promotes Cutaneous Squamous Cell Carcinoma (CSCC) through Targeting Nuclear Factor I/B (NFIB). PLoS ONE 9(6): e100620.

Zhou, W. and J. P. Thiery (2013). Loss of Git2 induces epithelial–mesenchymal transition by miR146a-Cnot6L-controlled expression of Zeb1. Journal of Cell Science 126(12): 2740-2746.

8 Acknowledgments

First and foremost, I would like to thank Prof. Stefan Engelhardt for giving me the opportunity to develop and write my doctoral thesis in his group. I would like to thank him for his continuous supervision, support, motivation and guidance over the whole period of this scientific work.

I would like to thank Prof. Alessandra Moretti for being my first mentor and for the chance to start a fruitful cooperation through this project. I would like to thank Prof. Thomas Meitinger for being my second mentor and his support in our meetings.

I wish to express my sincere thanks Dr. Yassine Sassi for all the practical training, the advices, the feedback and support day to day.

I would like to thank Petros Avramopoulos for supporting me and being such a great team player and lab mate.

I would like to thank Dr. Deepak Ramanujam for the practical training and counseling. Thanks to Cornelia Brönner and Sarah Hölscher for the orientation in the lab environment.

Thanks to Stanislas Werfel for providing me the double fluorescent reporter, the instruction of its use and the AAV9 construction reagents.

Thanks to Urszula Kremser for the preparation of the neonatal rat cardiomyocytes, Lucia Koblitz for the adult mouse preparations, Kornelija Sakac for the performed TAC operations and Sabine Brummer for the tissue sections and stainings.

I would also like to thank all other former and current members of the institute for their support and for creating such a comfortable working environment.

I wish to express my gratitude to my girlfriend for her support, patience, encouragement and help in innumerable challenging situations.

Finally, I would like to thank my family for their encouragement over this entire episode of my career and their unconditional support and love.